Ovarian Cancer Ascites Inhibits Transcriptional Activation of NK Cells Partly through CA125

Ovarian Cancer Ascites Inhibits Transcriptional Activation of Natural Killer Cells Partly Through CA125

Short running title: Inhibition of NK cells by ovarian cancer ascites

Authors: Christopher C. Fraser[1], Bin Jia[1], Guangan Hu[1], Lojain Ibrahim Al Johani[2], Roberta Fritz-Klaus[2], James Dongjoo Ham[1], Raina N. Fichorova[3], Kevin M. Elias[4], Daniel William Cramer[3], Manish S. Patankar[2], Jianzhu Chen[1]

[1]Koch Institute for Integrative Cancer Research and Department of Biology, Massachusetts Institute of Technology, Cambridge, Massachusetts, USA.
[2]Department of Obstetrics and Gynecology, University of Wisconsin-Madison, Madison, Wisconsin, USA.
[3]Department of Obstetrics, Gynecology and Reproductive Biology, Brigham and Women's Hospital, Harvard Medical School, Boston, Massachusetts, USA.
[4]Division of Gynecologic Oncology, Department of Obstetrics, Gynecology and Reproductive Biology, Brigham and Women's Hospital, Dana-Farber Cancer Institute, Harvard Medical School, Boston, Massachusetts, USA.

Christopher C. Fraser and Bin Jia contributed equally to this work.

Correspondence to:
Jianzhu Chen
Koch Institute for Integrative Cancer Research, MIT
500 Main St.
Cambridge MA, 02142
Telephone: 617-258-6173
email: jchen@mit.edu

The authors declare no potential conflicts of interest
Keywords: Ovarian cancer, ascites, Natural Killer (NK) cells, MUC16, CA125, transcriptional regulation

Abstract

Malignant ascites is a common clinical problem in ovarian cancer. Natural killer (NK) cells are present in the ascites but their anti-tumor activity is inhibited. The underlying mechanisms of the inhibition have yet to be fully elucidated. Using an Fcγ receptor-mediated NK cell activation assay, we show that ascites from ovarian cancer patients potently inhibits NK cell activation. Part of the inhibitory activity is mediated by CA125, a mucin 16 fragment shed from ovarian cancer tumors. Moreover, transcriptional analyses by RNA sequencing reveal up-regulation of genes involved in multiple metabolic pathways but down-regulation of genes involved in cytotoxicity and signaling pathways in NK cells purified from ovarian cancer patient ascites. Transcription of genes involved in cytotoxicity pathways are also down-regulated in NK cells from heathy donors following *in vitro* treatment with ascites or with a CA125 enriched protein fraction. These results show that ascites and CA125 inhibit anti-tumor activity of NK cells at transcriptional levels by suppressing expression of genes involved in NK cell activation and cytotoxicity. Our findings shed light on the molecular mechanisms by which ascites inhibits the activity of NK cells and suggest possible approaches to reactivate NK cells for ovarian cancer immunotherapy.

Key Points

1. NK cellular response is inhibited by ovarian cancer patient ascites.
2. Ascites alters NK cell gene expression involved in activation and cytotoxicity.
3. CA125, found in high concentration in ascites, inhibits NK cell function.

Introduction

Ovarian cancer is the leading cause of gynecologic cancer death in the United States and the fifth most common cancer-related cause of death in women, with over 22,000 new cases and greater than 14,000 deaths per year[1]. A major factor contributing to ovarian cancer morbidity is malignant ascites, the excess accumulation of fluid in the peritoneal cavity, occurring in more than one-third of patients[2,3]. Ascites in ovarian cancer patients may promote disease progression throughout the peritoneal cavity via the circulation of viable tumor spheroids[4,5,6]. From there the metastatic cells find other niches to grow, invade and increase tumor burden and physiological damage.

Many different cell types are found in ascites, including tumor cells, fibroblasts and immune cells, with lymphocytes and macrophages making up ~37% and ~32% respectively[7]. Although immune cells are abundant in the ascites, tumor growth remains unchecked. One hypothesis is immune suppression by regulatory T cells (T_{reg}), which are found in abundance in ascites of ovarian cancer patients[8]. There are multiple secreted factors in the ascites that may also inhibit immune responses, including factors such as IL-10[9], and IL-6, whose presence correlates with a poor prognosis and outcome[10]. Cytokine concentration in the ascites can exceed serum levels by over 1000-fold[11]. In addition to cytokines, other immune modulators such as chemokines[12] and matrix metallo-proteinases (MMPs)[13,14] influence tumor growth and metastasis in ascites[15,16,17].

Natural killer (NK) cells were originally identified as immune cells capable of killing tumor cells non-specifically. NK cell activation and tumor cell killing is regulated by a combination of activating and inhibitory signals. A number of mechanisms are known to control killing. These include recognition and lysis of tumor cells that have lost major histocompatibility complex (MHC) class I expression, or tumor cells that express stress induced ligands that are recognized by NK cell activating receptors. NK cells can also become activated through Fcγ receptor III (FcγRIII or CD16) to kill antibody-bound tumor cells, a phenomenon referred to as antibody-dependent cellular cytotoxicity (ADCC). Although NK cells are present in significant numbers in the ascites, their anti-tumor activity is inhibited by both soluble and membrane-bound factors[18]. It has been known for more than a decade that ascites can suppress immune cell activity[19,20], including NK cell function *in vitro* as assessed by tumor cell

killing[21]. NK cells purified from ascites have altered activity[22]. However, *in vitro* expanded NK cells derived from ascites are functional and can effectively kill autologous/allogeneic ovarian cancer cells[23,24,25], suggesting that the impaired activity is reversible.

One of the factors found in abundance in ovarian cancer ascites is mucin 16 (MUC16). MUC16 is a heavily glycosylated large transmembrane protein expressed by epithelial cells in mucosal tissues. MUC16 is shed from the cell surface through protease cleavage, especially under pathological conditions[26]. CA125 is a repetitive peptide epitope found in MUC16 that is recognized by the antibody OC125[27,28,29]. CA125 concentration in ascites fluid can be up to 130-fold higher than that found in serum and local CA125 concentration in tumors greatly exceeds that found in the serum of ovarian cancer patients[30]. For example, it has been shown that patients with levels of CA125 more than 100 U/mL in the serum can have local CA125 concentrations higher than 10,000 U/mL[31]. Because of the high concentrations associated with ovarian cancer, CA125 has been used as a clinical biomarker to monitor ovarian cancer progression[32,33,34], and anti-CA125 antibodies are being investigated as immune modulators[35,36].

One of the cellular targets that may be regulated by CA125 are NK cells. CA125-enriched protein fractions from ascites have been shown to inhibit NK cell activation *in vitro* as assessed by CD16 expression. CA125 has been shown to inhibit killing of ovarian and breast cancer cells by human NK cells[37,38,39]. One mechanism whereby CA125 can directly protect tumor cells from NK cell-mediated cytotoxicity is by preventing the formation of an immune synapse[38]. The role of CA125 in protecting tumor cells from NK killing is further shown by knock-down of CA125 expression in cancer cell lines resulting in increased NK cell-mediated killing[40]. Preliminary evidence suggests CA125 may interact with Siglec-9 and other lectins to inhibit NK cell activation and cytotoxicity. Despite this progress, the mechanisms by which ascites and CA125 inhibit NK cell activation and function are still largely unknown.

To address this question, we developed an FcγR-mediated NK cell activation assay where the effect of ascites and CA125 on NK cell activation can be readily measured by flow cytometry. We also analyzed genome-wide response of NK cells by RNA sequencing to ovarian cancer ascites *in vitro* and compared that response to NK cells purified directly from patient ascites. We show that ascites isolated from ovarian

cancer patients potently inhibits human NK cell activation *in vitro* and the inhibitory activity is partly due to CA125. Our results also show that both NK cell populations share down-regulation of NK cell activation and cytotoxicity pathways, which is also inhibited by *in vitro* treatment of NK cells with CA125-enriched fraction from ascites. These results show that ovarian cancer ascites and CA125 inhibit activation and cytotoxicity of human NK cells through transcriptional suppression and shed light on possible approaches to restore anti-tumor activity of NK cells for ovarian cancer immunotherapy.

Materials and Methods

Patient-derived ascites samples

Ascites samples were collected under IRB approved protocols 02-051 (Dana-Farber Cancer Institute), 2016P002742 (Brigham and Women's Hospital), or OS11702 (Department of Obstetrics and Gynecology, University of Wisconsin-Madison, Madison). Fluid samples represented either excess specimen collected during diagnostic procedures in the operating room or outpatient setting or samples collected during therapeutic paracenteses performed in the outpatient setting for recurrent ascites. All study subjects had advanced or recurrent gynecologic malignancies. In most cases this was Stage III or Stage IV high grade serous carcinoma or carcinosarcoma; otherwise, the histology was described clinically as Mullerian adenocarcinoma if classification to a precise histologic subtype was not possible. Samples were evenly divided between primary disease and recurrent cases. For assays requiring NK-cell retrieval, unspun samples were delivered fresh to the laboratory within 1 hour of collection. In cases where only the supernatant was required, samples were aliquoted into 50 ml conical tubes, then centrifuged at 580xg for 5 min in a 4 °C pre-cooled centrifuge to separate cell pellets from supernatant. Supernatants were stored at – 80 °C in 1 ml aliquots.

CA125 quantification

CA125 antigen detection assay was performed using a volume-efficient highly sensitive multiplex platform (Meso Scale Discovery (MSD), Gaithersburg, MD, USA) based on electrochemiluminescence (ECL) detection. CA125 levels in ascitic fluid were detected using Imager S600 (MSD) and a single-spot assay (MSD catalog number K151WC) with a linearity range of 0.6–10,000 U/ml. The ascitic fluid samples

were tested at multiple dilutions (1:10, 1:50 and 1:100). A positive quality control (QC) sample was run in duplicate on each ESL plate. The QC sample had a mean CA125 concentration of 1553.8 U/ml. The coefficient of variation was calculated as 100* (SD/average) for each assay plate and between plates. The intra-plate CV% was 11.7%. We have previously reported inter-plate CV of this assay of 9.1% to 19%[41,42].

MUC16 (CA125) enrichment

Fresh ascites from patients with advanced stage high grade serous ovarian cancer was centrifuged at 800xg for 30 min to remove the cellular components. The supernatant was processed to isolate MUC16 using a recently established protocol (Schuster-Little et al, manuscript submitted). Briefly, the ascites was sequentially filtered through No. 4, No. 6 and GF/F filters and the filtrate was concentrated using a Pelicon ultrafiltration cassette (1,000 kDa molecular cut-off). The retentate from the cassette was loaded on a Q-Sepharose ion exchange column (1.5 cm x 50 cm) that was washed with 10 mM Tris-HCL pH 7.0 followed sequential elution with this same buffer containing 200 mM sodium chloride and 4 M sodium chloride. The 4 M sodium chloride wash was concentrated by ultrafiltration and subjected to size exclusion chromatography on a Sepharose CL-4B column (1.5 cm x 50 cm) as described previously. The column was eluted with 10 mM ammonium bicarbonate and the first excluded peak was pooled and concentrated using a Centriprep (10 kDa molecular cut-off) cartridge (Amicon). The centriprep concentration also served as a buffer exchange step to remove ammonium bicarbonate buffer and to replace it with phosphate buffered saline for use in the cell culture assays. The purity of MUC16 was determined by monitoring for CA125 Units per milligram of total protein. The CA125 units were measured in the clinical pathology laboratory at the University of Wisconsin Hospital and Clinics using the Abbott (Architect) assay format and the total protein was measured using the Bicinchoninic acid assay (ThermoFisher). The MUC16 preparations that had a specific activity between 700,000- 1,500,000 U of CA125 per milligram of total protein were used in the biological assays.

Heat inactivation and antibody depletion of ascites and CA125 enriched protein fractions

Heat inactivation: ascites and protein fractions enriched for CA125 were heated at 95℃, 20 minutes. Antibody mediated CA125 depletion: anti-MUC16 antibody

(OC125) (Abcam, ab693) was added to ascites or CA125 fractions at a concentration of 1μg/ml. EZ-Link-NHS-PEG4-Biotin (Thermo Scientific) was added at a concentration of 10nmol/ml and incubated on ice for 2 hours or room temperature for 30 min, non-reacted biotin was removed by gel filtration. Streptavidin MicroBeads (Miltenyi Biotec) were added to samples, incubate 4-8℃ for 5 min in the dark then microbeads were removed by magnetic separation.

NK cell isolation from human peripheral blood mononuclear cells and ovarian cancer patient ascites

Human peripheral blood mononuclear cells (PBMCs) were isolated from normal donor blood (Research Blood Components, Cambridge, MA).100 mL blood was diluted 1:1 in phosphate buffered saline and then 35 ml overlaid on top of 12 ml Ficoll-Paque premium (GE Healthcare, Pittsburgh, PA) in a 50ml centrifuge tube. Tubes were spun at 1300 RPM for 30 min, and the transition phase PBMCs collected, diluted in PBS with 2% fetal calf serum and spun at 1200 rpm for 10 min. Cells were re-suspended in fetal bovine serum and 10% DMSO. PBMC were then immediately frozen at −80 ◦C and transferred to liquid nitrogen the following day. For NK cell isolation, frozen PBMCs were thawed, re-suspended in PBS with 10% fetal bovine serum (FBS), and spun down. NK cells were isolated using a human NK cell negative selection isolation kit (Stem Cell Technologies, Vancouver) according to manufacturer's instructions. To generate cytokine-induced memory-like (CIML) NK cells, the purified human primary NK cells were incubated overnight (12-16 hours) at 37°C in RPMI10 medium supplemented with a combination of rhIL-12 (10ng/mL, StemCell Technologies) + rhIL-15 (50ng/mL, StemCell Technologies) + rhIL-18 (50ng/mL, Life Technologies). The resulting CIML NK cells were used for cytotoxicity assays.

For NK cell isolation from ovarian cancer ascites, samples were spun at 450xg, 25ºC for 20 minutes and washed twice in in PBS with 2% FBS. Viable cells were counted by trypan blue exclusion. NK cells were isolated using EasySep™ Human NK Cell Isolation Kit (Stem Cell Technologies, Vancouver) according to manufacturer's instructions.

NK cell culture and flow cytometry

For CD107 staining, purified NK cells (2 X 10^5 cells in 200 µL/well) were plated in 96-well flat-bottom plate in the presence or absence of 10% ascites and incubated for 24 hours at 37°C and 5% CO2. After incubation, the NK cells were transferred to 96-well round-bottom plates. Separately, target cells (K562 or OVCAR-3) (ATCC) were stained with CellTracker™ Red (Thermo Fisher, Waltham, MA) (30 min at 37°C in 5% CO2 incubator). The stained target cells (2 X10^5 cells in 50µL) were added to the wells containing the control and ascites-treated NK cells. The anti-CD107a-PE was immediately added to the co-cultures, the plate was centrifuged (300 X g for 1 min) and incubated 37°C in 5% CO2 incubator for 1 h. After incubation, 1X Protein Transport Inhibitor cocktail (Thermo Fisher) was added, and the plate was incubated for an additional 3 hours. After incubation, cells were washed with phosphate buffered saline (PBS) containing 1% fetal bovine serum (FBS) and 1 X protein transport inhibitor cocktail. DAPI was added to the cells prior to flow cytometry analysis. Flow cytometry was performed on the Attune™ NxT cytometer (Thermo Fisher).

For intracellular IFN-γ staining purified NK cells (5 × 10^6 cells/mL) were incubated in media alone or in media containing 10% ascites for 24 hours at 37°C in 5% CO2 environment. K562 or OVCAR-3 targets (2 X 10^5 cells in 100 uL) were added to each well of a 96-well round-bottom plate. NK cells (1 X 10^5 per 100 uL) suspended in either NK medium or NK medium supplemented with 10% ascites were added to the target cells. Cells were centrifuged (30 X g for 3 min) incubated at 37°C for 1 h followed by the addition of 1x Protein Transport Inhibitor cocktail. After 5 h of incubation, cells were washed and stained with Ghost Dye™ Red 780 (Tonbo Biosciences San Diego, CA)

After additional washing, the cells were stained for anti-NKp46 (Anti-NKp46-APC (Clone 9E2/NKp46, BD Biosciences, Franklin Lakes, NJ), fixed using 4 X paraformaldehyde, permeabilized by incubation in PBS supplemented with 2% FBS, 2 mM EDTA, and 0.5% saponin buffer, and stored in the dark for 10 min at 4°C. The cells were then centrifuged and stained (30 min at 4°C in the dark) with anti-IFN-γ -PE (Clone B27, BD Biosciences). Cells were washed twice, resuspended in 200 µL staining solution, and analyzed by flow cytometry (Attune). All experiments were conducted in triplicate, and data were analyzed using unpaired parametric T-tests. Data were analyzed and plotted using the GraphPad Prizm software package.

For anti-body mediated NK cell activation, purified human NK cells were cultured in 96 well flat bottom plates in RPMI, 10% FBS, non-essential amino acids, sodium pyruvate, penicillin-streptomycin and β-mercaptoethanol (GIBCO). NK cells were plated at 1 x 10^5 / well and cultured in the presence or absence of ovarian cancer ascites in a final volume of 100 μL for 24 hours. NK cells were activated by addition of 100 mL of media containing 1 X 10^5 GMBL1 cells and 100 μg / ml rituximab (Roche). Cells were co-cultured for 24 hours and then stained with fluorochrome-conjugated antibodies: CD56 PE, 4-1BB APC, CD16 PE Cy7, and CD3 APC (Biolegend, San Diego, CA). Cells were then analyzed using either a FACSCanto or LSR2 flow cytometer (Becton-Dickenson) and data was analyzed using FlowJo. Statistics was performed using Prism softwear. GMBL1 cells are a human B cell leukemia/lymphoma line generated by transducing human CD34+ hematopoietic stem/progenitor cells with a lentivirus expressing GFP, c-myc and BCL-2 [43]. GMBL1 cells were expanded from a single clone.

NK / tumor cell cytotoxicity assays

For NK cell mediated K562 cell line killing, rested cytokine-induced memory-like (CIML) NK cells isolated from the peripheral blood of three donors were cultured with different amounts of an ascites mixture containing equal volume amounts of ascites from 5 different ovarian cancer patients. Cytokine-induced memory-like (CIML) NK cells were generated by pre-activating NK cells in rhIL-12 (10 ng/mL; Miltenyi Biotec), rhIL15 (50 ng/mL; Miltenyi Biotec), and rhIL18 (50 ng/mL; BioLegend) in NK MACS Medium (Miltenyi Biotec) supplemented with 10% heat-inactivated human AB serum (Sigma-Aldrich). After 16 hours, pre-activated NK cells were washed 3 times to remove cytokines and cultured in NK MACS medium containing 2 ng/mL rhIL-15.
48 hours later K562 target cells were added to the CIML NK cells at a E:T ratio of 1:1. Four hours after co-culture cytotoxicity was assessed by comparing viable K562 cells (DAPI-/Annexin V-) in each sample to a target-only control. For the GMBL1 killing assay, rested CIML NK cells isolated from the peripheral blood of four donors were cultured with different amounts of an ascites mixture containing equal volume amounts of ascites from 5 different ovarian cancer patients. 48 hours later GMBL1 target cells were added to the CIML NK cells at a E:T ratio of 1:2.5, with or without rituximab (f.c. 100 ng/mL). 6 hours after co-culture the % cytotoxicity was assessed by comparing

viable GMBL1 cells (DAPI-/Annexin V-) in each sample to a target-only control. Error bars shown are S.D.

Gene expression analysis by quantitative polymerase chain reaction

For quantitative RT-PCR (qRT-PCR) analysis, RNAs were extracted with RNeasy Micro kit (Qiagen), as per manufacturer's instructions. cDNA was generated with SuperScript First-Strand (Invitrogen), and quantitative PCR was performed using LightCycler 480 SYBR green mix (Roche). Primer sequences are shown in Supplemental Table 5.

RNA sequencing

RNAs were extracted with RNeasy MiniElute kit (Qiagen), converted into cDNA and sequenced using Next-Generation Sequencing (Illumina). RNAseq data was aligned to the human genome (version hg19) and raw counts of each gene of each sample were calculated with bowtie2 2.2.3[44] and RSEM 1.2.15[45]. Differential expression analysis was performed using the program edgeR at $P < 0.05$ with a 2-fold-change[46]. The gene expression level across different samples was normalized and quantified using the function of cpm. Differentially expressed genes were annotated using online functional enrichment analysis tool DAVID (http://david.ncifcrf.gov/)[47]. The heatmap was visualized with MeV[48]. Pathway image was drawn and modified by BioRender (https://biorender.com) based on the KEGG pathway (https://www.genome.jp/kegg/pathway.html).

Statistical Method

Statistical analysis was performed using GraphPad Prism (San Diego, CA).

Data availability

Raw sequences are deposited in the database of Gene Expression Omnibus (GEO) with accession ID: ID GSE153713. (https://www.ncbi.nlm.nih.gov/geo/query/acc.cgi?acc=GSM4650127).

Results

Human ovarian cancer ascites inhibits activation of NK cells

To test whether ascites may inhibit ADCC of NK cells, we established an *in vitro* assay where NK cells purified from heathy human donor blood were cultured with ascites for 24 hours and then co-cultured with a CD20-expressing human B cell leukemia line GMBL1 in the presence of anti-CD20 antibody rituximab (RTX) (Fig. 1a). NK cells from PBMCs express CD16 (FcγRIII) but not the co-stimulatory TNF-receptor family member 4-1BB (CD137, tumor necrosis factor receptor superfamily 9). Upon engagement of CD16 on NK cells with GMB1-bound RTX, NK cells are activated to express 4-1BB but down-regulate CD16 expression. We found that like freshly isolated NK cells from blood, NK cells expressed CD16 and little 4-1BB following co-culture with GMBL1 in the absence of RTX (Fig. 1b). As expected, NK cells lost CD16 but up-regulated 4-1BB following co-culture with GMBL1 in the presence of RTX. In contrast, if NK cells were pre-treated with ascites from ovarian cancer patients, the up-regulation of 4-1BB and down-regulation of CD16 were significantly attenuated.

To quantify the inhibitory activities of ascites, we cultured NK cells from 6 different donors with 1%, 10% or 30% ascites from 22 different ovarian cancer patients for 24 hours, then co-cultured with GMBL1 in the presence of RTX for another 24 hours, and measured 4-1BB and CD16 expression levels by flow cytometry. 4-1BB expression levels were increased sharply in all NK cell donors tested and the increase was inhibited by increasing percentages of ascites added into the culture (Fig. 1c). Conversely, a sharp reduction in CD16 expression levels was detected following FcγR-induced NK cell activation, which was inhibited by the increasing percentages of ascites added into the cultures (Fig. 1d). These results show that ascites contains factors that inhibit -mediated NK cell activation and effector function.

We also examined the effects of ascites on human NK cell activation by assaying CD107a and IFN-γ expression after stimulation with tumor cell lines. NK cells purified from multiple donor PBMCs were incubated with 10% ascites from multiple ovarian cancer patients for 24 hours and then stimulated with either OVCAR-3 or K562. The NK cell expression of CD107a and intracellular IFN-γ was assayed by flow cytometry 4-5 hours later. In all experiments, a consistent and statistically significant decrease in CD107a and intracellular IFN-γ expression was observed in NK cells that were pre-treated with ascites FcγR (Fig. 1e-f). Furthermore, we examined the effect of ascites in inhibiting NK cell cytotoxicity. For these experiments, NK cells isolated from donor PBMCs were treated with IL-15, IL-12 and IL-18 overnight to derived cytokine-

induced memory-like (CIML) NK cells[49,50]. CIML NK cells were then pre-treated with ascites pooled from 5 different ovarian cancer patients for 48 hours and used to kill K562 target cells or GMBL1 target cells with or without rituximab. As shown in Fig. 1 g-h, ascites pre-treatment of CIML NK cells significantly inhibited killing of K564 target cells as well as ADCC-mediated killing of GMBL1 target cells. Thus, ovarian cancer ascites inhibits NK cell activation and cytotoxicity mediated by FcγR and other activating receptors.

Purified CA125 inhibits FcγR-mediated NK cell activation

CA125 is abundant in ovarian cancer ascites and has been reported to inhibit NK cell activity *in vitro*[39]. To determine if CA125 might be responsible for the observed inhibitory activity of ascites in our FcγR-mediated NK cell activation assay, we purified a protein fraction (PE90) enriched in CA125 from two patient ascites by size-exclusion chromatography and measured CA125 and total protein concentrations (50,808 U/mL CA125, 640.6 μg/mL protein). We tested the effect of the purified CA125 on 4-1BB and CD16 expression as shown in Fig. 1a, replacing ascites with CA125 fraction PE90. 4-1BB up regulation was inhibited with increasing concentrations of purified CA125 fraction PE90 and was completely inhibited at 150 μg of PE90 (12,000 U/mL CA125) (Fig. 2a). However, purified CA125 fraction PE90 did not have any significant effect on CD16 expression even at the highest concentration added. This observation was extended when NK cells from three different donors were tested (Fig. 2b and data not shown).

We also tested a commercially purchased CA125 purified from an ovarian carcinoma cell line. Because azide was present in the commercial CA125, we tested CA125 before and after dialysis as well as azide alone in order to account for potential cellular effects of azide. As shown in Fig. 2c, 4-1BB was significantly inhibited by both dialized and non-dialized CA125 preparations, but not by azide alone. As with the CA125-enriched PE90 fraction, purified commercial CA125 had no significant effect on CD16 expression (Fig. 2d).

We also examined whether the inhibitory activity was heat-labile or could be attenuated by removing CA125 using an anti-CA125 antibody. CA125-enriched PE90 fraction and ascites were heat inactivated at 95℃ for 20 minutes or incubated with anti-CA125 antibody (OC125) followed by biotin/streptavidin microbeads and

magnetic separation. The heat inactivated (HI) or antibody (Ab)-treated PE90 or ascites were used to pretreat NK cells for 24 hours, followed by incubation with GBML1 and RTX and flow cytometry. Both heat inactivation and antibody-mediated CA125 depletion resulted in partial but significant, alleviation of the inhibitory activities of the CA125-enriched PE90 fraction and ascites (Fig. 2e,f). Together, these results show that CA125 derived from various sources is able to inhibit NK cell activation, and depletion of CA125 from a purified protein fraction or from ovarian cancer ascites partially blocked their inhibitory activity, suggesting that CA125 constitutes part of NK cell inhibitory factors in the ovarian cancer patient ascites.

Inhibition of NK cell activation is not correlated with CA125 concentration in ascites

To determine if inhibitory activity of ascites is correlated with CA125 concentration in the ascites, we measured the concentrations of CA125 in 22 ascites samples using a widely used clinical assay based on electrochemiluminescence (ECL) detection (Fig. 3a, Supplemental Table 1). Although addition of the higher percentage of ascites led to greater extent of inhibition of 4-1BB up-regulation and CD16 down-regulation (Fig. 1c,d and 2a,b), no correlation between the CA125 concentration in the ascites and the extent of inhibition of 4-1BB up-regulation or CD16 down-regulation was detected (Fig. 3b,c), suggesting the nature of the inhibitory activity is not entirely due to CA125, consistent with the only partial effect of purified CA125 on NK cell activation.

To identify other factors that may be correlated with NK cell inhibitory activity in the ascites, we measured a panel of factors known to inhibit NK cells, including MICA, MICB, IL-10, and TGF-β[41] in ascites from 11 patients by ELISA. Except for MICA, variable levels of MICB, IL-10 and TGF-β were detected in different ascites samples (Supplemental Table 2), but again there was no correlation between the levels of MICB, IL-10 or TGF-β and MFI of 4-1BB or CD16 expression on FcγR-activated NK cells (Supplemental Fig. 1). We also directly tested the effect of the ascites on CD16 expression on NK cells by culturing freshly purified NK cells from two different donors with ascites from 11 patients (in the absence of GMBL1 and RTX) for 72 hours. No significant alteration in CD16 expression was detected (Fig. 3d). Thus, CD16

expression does not seem to be inhibited by ascites in the absence of NK cell activation.

Exposure of NK cells to ascites leads to specific alteration in the transcriptome

To examine the effect of ascites on NK cells at the genome-wide level, we performed transcriptional analyses of NK cells with and without exposure to ascites by RNA sequencing (RNAseq). The samples included: 1) NK cells isolated from PBMCs of six healthy human donors cultured in media for 24 hours (healthy donor NK cells or HD), 2) NK cells from the same six healthy human donors but cultured with 30% ascites from two different ovarian cancer patients separately (ascites-treated NK cells or A1 and A2), and 3) NK cells purified directly from ascites of six different ovarian cancer patients (patient NK cells or PA). The purity of NK cells (>95% CD56+) and numbers of NK cells from 6 ascites are shown in Supplemental Fig. 2. RNA was isolated from the 24 samples and subjected to RNAseq. Principal component analyses showed that 6 healthy donor (HD) NK cell samples clustered together; 12 ascites-treated NK cell samples (A1 and A2) clustered together; and 6 patient ascites (PA) NK cell samples clustered together (Fig. 4a). These results suggest that most of the observed transcriptional changes are associated with the conditions under which the NK cells were exposed, with relatively low donor to donor variability.

Hierarchical clustering identified seven broad categories of gene expression patterns (Fig. 4b). These included transcripts that were up or down-regulated in both patient ascites and ascites treated NK cells (clusters C3 and C4). Detailed pathway analysis of differentially expressed genes (DEGs) revealed that a number of down regulated gene pathways involved in NK cell activation were conserved in both ascites-treated NK cells and patient ascites NK cells, including those involved in integrin signaling, leukocyte migration, NK cell cytotoxicity, adhesion, MAPK signaling, and cell activation (TCR/BCR). These data suggest that *in vitro* exposure of NK cells to ascites mimics exposure of NK cells to ascites *in vivo*, resulting in an immuno-suppressive state. Differential gene expression analysis between patient NK cells and healthy donor NK cells also revealed some remarkable changes (Fig. 4c and Supplemental Table 3). Genes that were differentially up-regulated in patient ascites NK cells were primarily involved in metabolic pathways, including oxidation-reduction, glycolysis, fatty acid beta-oxidation, carbon metabolism and amino sugar and nucleotide sugar metabolism. In contrast intracellular signal transduction pathways

were down-regulated in patient ascites NK cells, including type I interferon signaling, TCR, BCR, and phosphatidylinositol pathways. These results suggest that most of the observed transcriptional changes were linked to an activated metabolism and suppressed intracellular signaling pathways in patient NK cells.

Exposure of NK cells to ascites both *in vivo* and *in vitro* lead to transcriptional inhibition of cytotoxicity pathway

We further examined the transcriptomic differences and similarities between patient NK cells and ascites-treated NK cells. These two sources of NK cells had a significant number of DEGs in common that were either up or down regulated (444 and 312 genes, respectively) (Fig. 5a and Fig. 4b). Clustering analysis revealed similarities in many cellular processes (Fig. 5b). For example, patient NK cells and ascites-treated NK cells had in common up-regulation of gene expression in the inhibitory p53 pathway, whereas gene expression in both Wnt and Rap1 pathways were down-regulated (Fig. 5c, Supplemental Table 4). Several other gene sets relevant to NK cell function were also similarly inhibited including NK cell cytotoxicity, focal adhesion, and both MAPK, Wnt and TNF signaling. Overall the pattern of DEGs points to suppressed NK cell function when exposed to ascites.

We characterized the genes in the GO NK cytotoxicity pathway that were down regulated and shared between patient NK cells and ascites-treated NK cells (Fig. 6a). The most down-regulated genes included IFN-γ, KIR2DL1, KIR2DL3, KIR2DS4, HCST, ITGB2, and NCR3. To validate their differential expression, we quantified transcript levels of granzyme B (GZMB), integrin αL (ITGAL), integrin β2 (ITGB2), DAP10, ZAP70, phosphatidylinositol 3-kinase regulatory subunit β (PIK3R1), NKp30, and NKp46 by quantitative PCR (qPCR). The results confirmed down-regulation of these transcripts in patient NK cells (Fig. 6b). Down-regulation of these transcripts in ascites-treated NK cells was less pronounced but still significant, with the largest differences in expression compared to healthy donors being ITGB2 and NKp30. In addition, we treated freshly isolated NK cells from two healthy donors with CA125-enriched fraction P1 isolated from ascites of an ovarian cancer patient for 24 hours, isolated RNA and performed qPCR. As shown in Fig. 6b, CA125 treatment also down-regulated the levels of all eight transcripts, suggesting that CA125 contributes partly to the transcriptional inhibition in NK cells.

Based on data from the transcriptomic analysis, we defined the specific genes in the NK cell cytotoxic pathways that were similarly down-regulated in patient NK cells and ascites-treated NK cells (Fig. 6c, Supplemental Fig. 3). These included NK cell activation receptors, such as NKp30, NKp46, KIR2DL, ITGAL and ITGB2; intracellular molecules, such as DAP10, ZAP70, PI3K, RAC and PKC, involved in NK cell signaling and activation; and effector molecules, such as IFN-γ, granzyme B and perforin, involved in killing target cells. Additional cell surface receptors and intracellular signaling molecules, such as NKG2D, 4B4, NKp46, KIR2DS, CD94, LCK, LAT, 3BP2, and NFAT, were down-regulated in patient NK cells but not in ascites-treated NK cells. These results show that transcriptional activation of cytotoxicity and signaling pathways is inhibited in NK cells from patient ascites and following ascites-treatment *in vitro*.

Discussion

Malignant ascites is a major factor contributing to ovarian cancer recurrence and mortality. Ovarian cancer ascites contains immune cells and soluble factors that can inhibit cellular immune response *in vitro*[8,9]. NK cells, which normally exhibit potent tumoricidal activity, are one of the immune cell types found in ascites. In order to evaluate if ascites can suppress NK cell functional response, we used a cell based assay where NK cells are activated by FcγRIII (CD16) cross-linking to cell-bound antibody complexes. The approach is significantly different from those used in the past to test for inhibitory activity of ascites because it is mediated by antibody bound tumor cells, and the read out is up-regulation of 4-1BB, analyzed 24 hours after stimulation. In contrast, in previously published assays NK cells were cultured without stimulation for 72 hours and then analyzed for CD16 expression[39]. The assay we employed requires both cells expressing the antigen (in this case CD20 on GMBL1 cells) and an antigen-specific antibody (anti-CD20 or rituximab). Antibody binding to the FcγRIII on NK cells results in up-regulation of the co-stimulatory molecule 4-1BB and down regulation of CD16. Our results show that ascites inhibit FcγR-mediated NK cell activation.

CA125 is found at high but variable concentrations in ascites and has been shown to inhibit NK cell activity *in vitro*, and that incubation of NK cells with purified CA125 *in vitro* without additional stimulation down regulated CD16 and inhibited NK

cell tumoricidal activity[39]. We observed that CA125 purified from ovarian cancer patient ascites and from an ovarian cancer cell line inhibited FcγR-mediated NK cell activation as assessed by up regulation of 4-1BB. Conversely, NK cell inhibitory activity could be partially removed by CA125 depletion and heat inactivation. It has been reported that a role of CA125 in inhibiting NK cell ADCC was mediated by suppressing FcγR engagement by antibodies[51]. Although we did not observe down regulation of CD16 expression in response to FcγR-mediated NK cell activation with purified CA125, CD16 down-regulation was inhibited by ascites. These results suggest that there are likely additional factors in the ascites that inhibit different aspects of NK cell activation and function.

We observed a dosage-dependent inhibition of 4-1BB up-regulation or CD16 down-regulation on NK cells when cultured with ascites. However, we found no correlation between concentration of CA125 in the ascites and up-regulation of 4-1BB or down-regulation of CD16 on NK cells. The lack of correlation may highlight the limit of knowledge regarding the potential active forms of MUC16-derived CA125, in that the protein detection assay may not fully reflect the concentration of the biologically active form. This notion is consistent with the presence of additional factors other than CA125 in the ascites that modulate CD16 expression on NK cells. Attempts to target CA125 using antibody therapeutics has limited success[52,53]. Among potential explanations for the failure is lack of understanding of MUC16 biology, for example kinetics, cleavage and shedding[54,55] have yet to be fully understood. It is also possible that inhibition is mediated by a CA125-interacting protein, glycan or lipid, rather than CA125 itself.

To further investigate the mechanisms by which ascites and CA125 inhibit NK cell activation and function, we examined at the whole genome-level transcriptional changes by RNAseq and compared NK cells from healthy donors with or without ascites treatment for 24 hours and NK cells purified from ovarian cancer patient ascites. NK cells derived from multiple donors had similar overall RNA profiles suggesting the dominant effect of ascites on NK cells over individual variations among patients. Considering ovarian cancer ascites contains various number of tumor cells and immune cells, and various concentrations of cytokines, chemokines and proteases[3], it is therefore surprising that we found consistency among multiple donor NK cells, whether isolated directly from ascites, or cultured *in vitro*. The RNA profile of

NK cells purified directly from ascites was profoundly different from that of normal donor NK cells purified from peripheral blood. Among the up-regulated genes, many are involved in metabolic pathways of amino acids, nucleotides, sugar, and fatty acids. Because cellular metabolism is required for normal NK cell function[56], the transcriptional changes in a large number of metabolic pathways in patient NK cells are striking and suggest NK cells from ascites are wired differently from those of normal NK cells from blood.

Among the down-regulated genes in NK cells from ascites, many are involved in NK cell cytotoxicity, MAPK, RAP1 and Wnt signaling pathways. Notably, the same pathways are also down-regulated when NK cells were treated with ascites *in vitro* for just 24 hours. These results suggest that transcriptional down-regulation of cytotoxicity and various signaling pathways is rapid in NK cell following exposure to ascites. They also underlie the molecular mechanisms through which ascites inhibit NK cell activation and function. Furthermore, eight of the selected genes in NK cell cytotoxicity pathways were also rapidly down-regulated upon treatment of healthy donor NK cells with a CA125 fraction for 24 hours, suggesting that CA125 also inhibits NK cell activity through the same mechanism. Our findings reveal molecular mechanisms by which ascites and CA125 inhibit NK cell activation and function and shed light on how to reverse NK cell activity for ovarian cancer immunotherapy.

Acknowledgements

The authors thank Koch Institute Swanson Biotechnology Center and core facilities for assistance with flow cytometry and RNA-seq data acquisition and analysis. The authors would like to thank the DFCI Gyn CRIS team, Isha Lokurka, Dr. Dipanjan Chowdhury, and Dr. Rajeshwari Kalyanaraman for assistance with ascites acquisition. The authors would also like to thank Khaing Thazin for assistance with NK cell culture experiments.

Funding

This work was supported in part by National Institutes of Health Grants CA197605 (to DWC), the Koch Institute Support (core) Grant P30-CA14051 from the National Cancer Institute, Ivan R. Cottrell Research Fund, and the Brigham Ovarian Cancer Research Fund (KME).

References

1. Siegel, R.L., K.D. Miller, and A. Jemal. 2020. Cancer statistics. CA Cancer J. Clin. 70: 7-30.

2. Smolle, E., V. Taucher, and J. Haybaeck. 2014. Malignant ascites in ovarian cancer and the role of targeted therapeutics. Anticancer Res. **34**:1553-1561.

3. Kipps, E., D.S. Tan, and S.B. Kaye. 2013. Meeting the challenge of ascites in ovarian cancer: new avenues for therapy and research. Nature Rev. Cancer 13: 273–282.

4. Burleson, K.M, M.P. Boente, S.E. Pambuccian, and A.P. Skubitz. 2006. Disaggregation and invasion of ovarian carcinoma ascites spheroids. J. Transl. Med. 4: 6.

5. Shield, K., M.L. Ackland, N. Ahmed, and G.E. Rice. 2009. Multicellular spheroids in ovarian cancer metastases: Biology and pathology. Gynecol. Oncol. 113: 143-148.

6. Davidowitz, R.A., L. M. Selfors, M.P. Iwanicki, K.M. Elias, A. Karst, H. Piao, T.A. Ince, M.G. Drage, J. Dering, G.E. Konecny, U. Matulonis, G.B. Mills, D.J. Slamon, R. Drapkin, and J.S. Brugge. 2014. Mesenchymal gene program-expressing ovarian cancer spheroids exhibit enhanced mesothelial clearance. J. Clin. Invest. 124: 2611-2625.

7. Sheid, B. 1992. Angiogenic effects of macrophages isolated from ascitic fluid aspirated from women with advanced ovarian cancer. Cancer Lett. 62:153–158.

8. Johannes Landskron, J., Ø. Helland, K.M. Torgersen, E.M. Aandahl, B.T. Gjertsen, L. Bjørge, and K. Taskén. 2015. Activated regulatory and memory T-cells accumulate in malignant ascites from ovarian carcinoma patients. 2015. Cancer Immunol. Immunother. 64: 337- 347.

9. Matte, I., D. Lane, C. Laplante, C. Rancourt, and A. Piché. 2012. Profiling of cytokines in human epithelial ovarian cancer ascites. Am. J. Cancer Res. 2: 566-580.

10. Lane, D., I. Matte, C. Rancourt, and A. Piche. 2011. Prognostic significance of IL-6 and IL-8 ascites levels in ovarian cancer patients. BMC Cancer. 11: 210.

11. Penson, R.T., K. Kronish, Z. Duan, A.J. Feller, P. Stark, S. E. Cook, L.R. Duska, A.F. Fuller, A.K. Goodman, N. Nikrui, K.M. MacNeill, U.A. Matulonis, F.I. Preffer, and M.V. Seiden. 2000. Cytokines IL-1β, IL-2, IL-6, IL-8, MCP-1, GM-CSF and TNF-α in patients with epithelial ovarian cancer and their relationship to treatment with paclitaxel. Int. J. Gynecol. Cancer. 10: 33–41.

12. Milliken, D., C. Scotton, S. Raju, F. Balkwill, and Julia Wilson. 2002. Analysis of chemokines and chemokine receptor expression in ovarian cancer ascites. Clin. Cancer Res. 8: 1108-1114.

13. Belotti, D., P. Paganoni, L. Manenti, A. Garofalo, S. Marchini, G. Taraboletti, and R. Giavazzi. 2003. Matrix metalloproteinases (MMP9 and MMP2) induce the release of vascular endothelial growth factor (VEGF) by ovarian carcinoma cells: implications for ascites formation. Cancer Res. 63: 5224–5229.

14. Yokoi, A., Y. Yoshioka, Y. Yamamoto, M. Ishikawa, S. Ikeda, T. Kato, T. Kiyono, F. Takeshita, H. Kajiyama, F. Kikkawa and T. Ochiya. 2017. Malignant extracellular vesicles carrying MMP1 mRNA facilitate peritoneal dissemination in ovarian cancer. Nat Commun. 8:14470.

15. Lane, D., V. Robert, R Grondin, C. Rancourt, and A. Piche. 2007. Malignant ascites protect against TRAIL- induced apoptosis by activating the PI3K/Akt pathway in human ovarian carcinoma cells. Int. J. Cancer. 121: 1227–1237.

16. Lane, D., N. Goncharenko-Khaider, C. Rancourt and A. Piche. 2010. Ovarian cancer ascites protects from TRAIL-induced cell death through αvβ5 integrin-mediated focal adhesion kinase and Akt activation. Oncogene. 29: 3519–3531.

661 17. N. Goncharenko-Khaider, I. Matte, D. Lane, C. Rancourt, and A. Piche. 2012.
662 Ovarian cancer ascites increase Mcl-1 expression in tumor cells through ERK1/2-
663 Elk-1 signaling to attenuate TRAIL-induced apoptosis. Mol. Cancer. 1166: 84.
664
665 18. Morvan, M.G., and L.L. Lanier. 2016. NK cells and cancer: you can teach innate
666 cells new tricks. Nat. Rev. Cancer.16: 7-19.
667
668 19. Badger, A.M., S.R. Cooperband, V.J. Merluzzi, and A.H. Glasgow. 1977.
669 Immunosuppressive activity of ascitic fluids from patients with cancer metastatic to
670 the peritoneum. Cancer Res. 37: 1220-1226.
671
672 20. Hess, A.D., S.A. Gall, and J.R. Dawson. 1979. Inhibition of *in vitro* lymphocyte
673 function by ascitic fluids from ovarian cancer patients. Cancer Res. 39: 2381-2389.
674
675 21. Onsrud, M. 1986. Immunosuppressive effects of peritoneal fluids from ovarian
676 cancer patients. Gynecologic Oncology. 23: 316-322.
677
678 22. Belisle, J.A., J.A.A. Gubbels, C.A. Raphael, M. Migneault, C. Rancourt, J.P.
679 Connor, and M.S. Patankar. 2007. Peritoneal natural killer cells from epithelial
680 ovarian cancer patients show an altered phenotype and bind to the tumour marker
681 MUC16 (CA125). Immunology. 122: 418–429.
682
683 23. Belisle, J.A., J.A.A. Gubbels, C.A. Raphael, M. Migneault, C. Rancourt, J.P.
684 Connor, and M.S. Patankar. 2018. Ex vivo-expanded NK cells from blood and
685 ascites of ovarian cancer patients are cytotoxic against autologous primary ovarian
686 cancer cells. Cancer Immunol. Immunother. 67: 575-587.
687
688 24. Felices, M., S. Chu, B. Kodal, L. Bendzick, C. Ryan, A. J. Lenvik, K. L. M.
689 Boylan, H. C. Wong, A. P. N. Skubitz, J. S. Miller, and M. A. Geller. 2017. IL-15
690 super-agonist (ALT-803) enhances natural killer (NK) cell function against ovarian
691 cancer. Gynecol. Oncol. 145: 453–461.
692
693 25. Hoogstad-van Evert, J.S., R.J. Maas, J. van der Meer, J. Cany, S. van der Steen,
694 J.H. Jansen, J.S. Miller, S. Bekkers, W. Hobo, L. Massuger, and H. Dolstra. 2018

695 Peritoneal NK cells are responsive to IL-15 and percentages are correlated with
696 outcome in advanced ovarian cancer patients. Oncotarget. 9: 34810-34820.
697
698 26. Govindarajan, B., B.B.Menon, S. Spurr-Michaud, K. Rastogi, M.S. Gilmore, P.
699 Argüeso, and I.K. Gipson. 2012. A metalloproteinase secreted by Streptococcus
700 pneumoniae removes membrane mucin MUC16 from the epithelial glycocalyx
701 barrier. PLoS One. 7**:** e32418.
702
703 27. O'Brien, T.J., J.B. Beard, L.J. Underwood, R.A. Dennis, A.D. Santin, and L. York.
704 2001. The CA125 gene: an extracellular superstructure dominated by repeat
705 sequences. Tumour Biol. 22: 348–366.
706
707 28. Yin, B.W., and K.O. Lloyd. 2001. Molecular cloning of the ca125 ovarian cancer
708 antigen. identification as a new mucin, muc16. J. Biol. Chem. 276: 27371–27375.
709
710 29. Fleuren, G.J., M. Nap, J.G. Aalders, J.B. Trimbos, and H.W. de Bruijn. 1987.
711 Explanation of the limited correlation between tumor CA 125 content and serum CA
712 125 antigen levels in patients with ovarian tumors. Cancer. 60: 2437-2442.
713
714 30. Serreyn, R., J. Deboever, G. Martens, and D. Vandekerckhove.1991.
715 Quantitative assessment of CA-125 in the normal ovary and in benign and malignant
716 ovarian tumours. J. Tumor Marker Oncol. 5: 341–349.
717
718 31. Crombach, G., A. Scharl, and H. Würz. 1989. CA125 in normal tissues and
719 carcinomas of the uterine cervix, endometrium and Fallopian tube. II.
720 Immunoradiometric determination in secretions, tissue extracts and serum. *Arch.*
721 Gynecol. Obstet. 244: 113–122.
722
723 32. Felder, M., A. Kapur, J. Gonzalez-Bosquet, S. Horibata, J. Heintz, R. Albrecht, L.
724 Fass, J. Kaur, K. Hu, H. Shojaei, R.J. Whelan, and M.S. Patankar.2014. MUC16
725 (CA125): tumor biomarker to cancer therapy, a work in progress. Mol. Cancer.
726 13:129.
727

728 33. Duffy, M.J., J.M. Bonfrer, J. Kulpa, G.J.S. Rustin, G. Soletormos, G.C. Torre,
729 M.K. Tuxen, and M. Zwirner. 2005. CA125 in ovarian cancer: European group on
730 tumor markers guidelines for clinical use. Int. J. Gynecol. Cancer 15: 679–691.
731
732 34. Sturgeon, C.M., M.J. Duffy, U-H. Stenman, H. Lilja, N. Brünner, D.W. Chan,
733 R. Babaian, R.C. Bast Jr., B. Dowell, F.J. Esteva, C. Haglund, N. Harbeck, D.F.
734 Hayes, M. Holten-Andersen, G.G. Klee, R. Lamerz, L.H. Looijenga, R. Molina,
735 H.J. Nielsen, H. Rittenhouse, A. Semjonow, I-M. Shih, P. Sibley, G. Sölétormos,
736 C. Stephan, L. Sokoll, B.R. Hoffman, and E.P. Diamandis. 2008. National
737 Academy of Clinical Biochemistry. National Academy of Clinical Biochemistry
738 laboratory medicine practice guidelines for use of tumor markers in testicular,
739 prostate, colorectal, breast, and ovarian cancers. Clin. Chem. 54: e11–e79.
740
741 35. No authors listed. 2006. Oregovomab. anti-CA-125 monoclonal antibody
742 B43.13--AltaRex, B43.13, MAb B43.13, monoclonal antibody B43.13. Drugs R. D. 7:
743 379-383.
744
745 36. Battaglia, A., A. Buzzonetti, M. Fossati, G. Scambia, A. Fattorossi, M.R.
746 Madiyalakan, Y.D. Mahnke, and C. Nicodemus. 2020. Translational immune
747 correlates of indirect antibody immunization in a randomized phase II study using
748 scheduled combination therapy with carboplatin/paclitaxel plus oregovomab in
749 ovarian cancer patients. Cancer Immunol Immunother. 69: 383-397.
750
751 37. Belisle, J.A., S. Horibata, G.A. Jennifer, S. Petrie, A. Kapur, S. André, H.J.
752 Gabius, C. Rancourt, J. Connor, J.C. Paulson, and M.S. Patankar. 2010.
753 Identification of Siglec-9 as the receptor for MUC16 on human NK cells, B cells, and
754 monocytes. Mol. Cancer 9: 118.
755
756 38. Gubbels, J.A.A., M. Felder, S. Horibata, J.A. Belisle, A. Kapur, H. Holden, S.
757 Petrie, M. Migneault, C. Rancourt, J.P. Connor, and M.S. Patankar. 2010. MUC16
758 provides immune protection by inhibiting synapse formation between NK and ovarian
759 tumor cells. Mol. Cancer 9:11.
760

761 39. Patankar, M.S., Y. Jing, J.C. Morrison, J.A. Belisle, F.A. Lattanzio, Y. Deng, N.K.
762 Wong, H.R. Morris, A. Dell, and G.F. Clark. 2005. Potent suppression of natural killer
763 cell response mediated by the ovarian tumor marker CA125. Gynecol. Oncol. 99:
764 704–713.
765
766 40. Felder, M., A. Kapur, A.L. Rakhmilevich, X. Qu, P.M. Sondel, S.D. Gillies, J.
767 Connor, and M.S. Patankar. 2019. MUC16 suppresses human and murine innate
768 immune responses. Gynecol. Oncol.152: 618-628.
769
770 41. Cramer, D. W., A.F. Vitonis, S.P. Pinheiro, J.R. McKolanis, R.N. Fichorova, K.E.
771 Brown, T.F. Hatchette, and O.J. Finn. 2010. Mumps and ovarian cancer: modern
772 interpretation of an historic association. Cancer Causes & Control. 21:1193–1201.
773
774 42. Fortner, R. T., A.F. Vitonis, H. Schock, A. Hüsing, T. Johnson, R.N. Fichorova, T.
775 Fashemi, H.S. Yamamoto, A. Tjønneland, L. Hansen, K. Overvad, M.C. Boutron-
776 Ruault, M. Kvaskoff, G. Severi, H. Boeing, A. Trichopoulou, V. Benetou, C. La
777 Vecchia, D. Palli, S. Sieri, R. Tumino, G. Matullo, A. Mattiello, N.C. Onland-Moret,
778 P.H. Peeters, E. Weiderpass, I.T. Gram, M. Jareid, J.R. Quirós, E.J. Duell, M.J.
779 Sánchez, M.D Chirlaque, E. Ardanaz, N. Larrañaga, B. Nodin, J. Brändstedt, A.
780 Idahl, K.T. Khaw, N. Allen, M. Gunter, M. Johansson, L. Dossus, M.A. Merritt, E.
781 Riboli, D.W. Cramer, R. Kaaks, and K.L.Terry. 2017. Correlates of circulating ovarian
782 cancer early detection markers and their contribution to discrimination of early
783 detection models: results from the EPIC cohort. J. Ovarian Res. 10: 20.
784
785 43. Leskov, I., C.P. Pallasch, A. Drake, B.P. Iliopoulou, A. Souza, C.H. Shen, C.D.
786 Schweighofer, L. Abruzzo, L.P. Frenzel, C.M. Wendtner, M.T. Hemann, and J. Chen.
787 2013. Rapid generation of human B-cell lymphomas via combined expression of Myc
788 and Bcl2 and their use as a preclinical model for biological therapies. Oncogene
789 32:1066-1072.
790
791 44. Langmead, B., C. Trapnell, M. Pop, and S.L. Salzberg. 2009. Ultrafast and
792 memory-efficient alignment of short DNA sequences to the human genome. Genome
793 Biol. 10: R25.
794

45. Li, B. and C.N. Dewey. 2011. RSEM: accurate transcript quantification from RNA-Seq data with or without a reference genome. BMC Bioinformatics 12, 323.

46. Robinson, M. D., D.J. McCarthy, and G.K. Smyth. 2010. edgeR: a Bioconductor package for differential expression analysis of digital gene expression data. Bioinformatics 26: 139–140.

47. Huang, D. W., B.T. Sherman, Q. Tan, J.R. Collins, W.G. Alvord, J. Roayaei, R. Stephens, M.W. Baseler, H.C. Lane, and R.A. Lempicki. 2007. The DAVID Gene Functional Classification Tool: a novel biological module-centric algorithm to functionally analyze large gene lists. Genome Biology. 8: R183.

48. Saeed, A. I., V. Sharov, J. White, J. Li, W. Liang, N. Bhagabati, J. Braisted, M. Klapa, T. Currier, M. Thiagarajan, A. Sturn, M. Snuffin, A. Rezantsev, D. Popov, A. Ryltsov, E. Kostukovich, I. Borisovsky, Z. Liu, A. Vinsavich, V. Trush, and J. Quackenbush. 2003. TM4: a free, open-source system for microarray data management and analysis. BioTechniques 34: 374–378.

49. Romee, R., M. Rosario, M.M. Berrien-Elliott, J.A. Wagner, B.A. Jewell, T. Schappe, J.W. Leong, S. Abdel-Latif, S.E. Schneider, S. Willey, C.C. Neal, L. Yu, S.T. Oh, Y.S. Lee, A. Mulder, F. Claas, M.A. Cooper, and T.A. Fehniger. 2016. Cytokine-induced memory-like natural killer cells exhibit enhanced responses against myeloid leukemia. Sci. Transl. Med. 8: 357ra123 .

50. Tarannum, M., and R. Romee. 2021. Cytokine-induced memory-like natural killer cells for cancer immunotherapy. Stem Cell Res.Ther.12: 592.

51. Kline, J.B., R.P. Kennedy, E. Albone, Q. Chao, S. Fernando, J.M. McDonough, K. Rybinski, W. Wang, E.B. Somers, C. Schweizer, L. Grasso, and N.C. Nicolaides. 2017. Tumor antigen CA125 suppresses antibody-dependent cellular cytotoxicity (ADCC) via direct antibody binding and suppressed Fc-γ receptor engagement. Oncotarget. 8: 52045-52060.

52. Berek, J.S., P.T. Taylor, A. Gordon, M.J. Cunningham, N. Finkler, J. Orr Jr., S. Rivkin, B.C. Schultes, T.L. Whiteside, and C.F. Nicodemus. 2004. Randomized, placebo-controlled study of oregovomab for consolidation of clinical remission in patients with advanced ovarian cancer. J. Clin. Oncol. 22: 3507–3516.

53. Sabbatini, P., P. Harter, G. Scambia, J. Sehouli, W. Meier, P. Wimberger, K.H. Baumann, C. Kurzeder, B. Schmalfeldt, D. Cibula, M. Bidzinski, A. Casado, A. Martoni, N. Colombo, R.W. Holloway, L. Selvaggi, A. Li, J. del Campo, K. Cwiertka, T. Pinter, J.B. Vermorken, E. Pujade-Lauraine, S. Scartoni, M. Bertolotti, C. Simonelli, A. Capriati, C.A. Maggi, J.S. Berek, and J. Pfisterer. 2013. Abagovomab as maintenance therapy in patients with epithelial ovarian cancer: a phase III trial of the AGO OVAR, COGI, GINECO, and GEICO–the MIMOSA study. J. Clin. Oncol. 31:1554–1561.

54. Das, S.,and S.K. Batra. 2015. Understanding the unique attributes of MUC16 (CA125): Potential implications in targeted therapy. Cancer Res. 75: 4669.

55. Aithal, A., S. Rauth, P. Kshirsagar, A. Shah, I. Lakshmanan, W.M. Junker, M. Jain, M.P. Ponnusamy, and S.K. Batra. 2018. MUC16 as a novel target for cancer therapy. Expert Opin. Ther. Targets 22: 675-686.

56. O'Brien, K.L, and D.K. Finlay. 2019. Immunometabolism and natural killer cell responses. Nat. Rev. Immunol.19: 282-290.

Figure Legends

Figure 1. Ascites from human ovarian cancer patients inhibits FcγR-mediated NK cell activation *in vitro*. a, Schematic of the assay used to evaluate inhibition of NK cells *in vitro*. Human NK cells are purified from PBMCs of healthy donors and pre-treated for 24 hours in the presence or absence of ascites. To activate NK cells, rituximab (RTX) and the CD20+ lymphoma cell line GMBL1 are added and the cells

are cultured for another 24 hours. CD16 and 4-1BB expression are analyzed using flow cytometry. Naïve NK cells express CD16 but little 4-1BB and activated NK cells express 4-1BB but down-regulate CD16. **b,** Representative flow cytometry analysis of 4-1BB and CD16 expression on NK cells incubated with GMBL1 alone (no ascites pre-treatment and no RTX), or incubated with GMBL1 and RTX (no ascites pre-treatment), or pre-treated with 30% ascites followed by incubation with GMBL1 and RTX. Live NK cells (CD56+ GFP- DAPI-) are gated free of GFP+ GMBL1 lymphoma cells and then analyzed for CD16 or 4-1BB expression. The numbers indicate mean fluorescent intensity (MFI). **c** and **d,** Compilation of the effects of different percentages of ascites from 22 ovarian patients on 4-1BB (**c**) and CD16 (**d**) expression on NK cells from 6 different donors. NS: NK cells were incubated with GMBL1 alone without ascites pre-treatment nor RTX (negative control); RTX: NK cells were incubated with GMBL1 and RTX without ascites pre-treatment (positive control); 1, 10 and 30: NK cells were pre-treated with 1%, 10% or 30% ascites from 22 ovarian cancer patients for 24 hours and then incubated with GMBL1 cells and RTX for another 24 hours. Flow cytometry analyses were done in the same way as in b. Each dot represents MFI of 4-1BB or CD16 of one NK cell sample. **e** and **f**, Human NK cells were purified from PBMCs of healthy donors and pre-treated for 24 hours in the presence or absence of 10% ascites (ASC). OVCAR-3 cells (**e**) or K562 cells (**f**) were then added to the NK cell cultures for 4-5 hours and NK cells were analyzed by flow cytometry for expression of intracellular IFN-γ or CD107. NK cells from 3 different PBMC donors and ascites from 3 different patients were assayed in response to OVCAR-3 and NK cells from 6 different PBMC donors and ascites from 5 different patients were assayed in response to K562. All experiments were done in triplicate. Data shown are compilation of results from different donors and ascites. **g** and **h**, NK cells isolated from PBMC donors were treated overnight with IL-15, IL-12 and IL-18 and then cultured with an ascites mixture from 5 different patients for 48 hours. K562 target cells were added at a E:T ratio of 1:1 and 4 hours later cytotoxicity was assessed by comparing viable K562 cells (DAPI-/Annexin V-) in each sample to a target-only control (**g**). Or GMBL1 target cells were added to the NK cell culture at a E:T ratio of 1:2.5, with or without rituximab and 6 hours later cytotoxicity was assessed by comparing viable

GMBL1 cells (DAPI-/Annexin V-) in each sample to a target-only control (**h**). All experiments were done in triplicate. Shown are results of NK cells isolated from three (**g**) or four (**h**) PBMC donors. Each line represents a different NK cell donor. Error bars are standard deviation. Statistical analysis was performed using one-way Anova (a-b) and an unpaired T-test (e-h). *p<0.01, **p<0.001, ***p<0.0001 comparing MFI of the indicated samples.

Figure 2. CA125 is partially responsible for NK cell inhibitory activity of ascites. **a,** Representative flow cytometry analyses of 4-1BB and CD16 by NK cells with and without pretreatment with CA125-enriched protein fraction PE90 from ascites. The same as in Fig. 1a, freshly purified human NK cells were cultured for 24 hours with or without 5, 50 and 150 μg of PE90 (400, 4000 and 12000 U CA125 respectively). Then, GMBL1 and/or RTX were added into the culture and incubated for another 24 hours followed by flow cytometry. The numbers indicate MFI. **b**, Comparison of MFI of 4-1BB on NK cells from three different donors with or without pre-treatment with different amount of PE90 for 24 hours prior to stimulation with GMBL1 and/or RTX. **c** and **d**, Comparison of MFI of 4-1BB (**c**) and CD16 (**d**) on NK cells from three different donors with or without pretreatment with dialyzed and non-dialyzed commercial CA125 (0.1% azide stock) or with dialyzed and non-dialyzed 0.1% azide stock in PBS. The final concentration of azide in cultures was 0.03% for both CA125 or azide alone cultures. NS: no pretreatment; PBS; pretreatment with PBS; AZ: pretreatment with azide; CA125: pretreatment with commercially purified CA125 (17kU/mL); dAZ: pretreatment with dialyzed azide (against PBS); dCA125: pretreatment with commercially purified CA125 dialyzed against PBS. **e**, The effect of heat and anti-CD125 antibody treatment of CA125-enriched fraction PE90 on 41-BB expression in the ADCC-mediated NK cell activation assay. PE90 fraction was heat inactivated at 95℃ for 20 minutes (PE90 HI) or incubated with anti-CA125 antibody (OC125) followed by EZ-Link-NHS-PEG4-Biotin, streptavidin microbeads and magnetic separation to remove CA125 (PE90 Ab). NK cells from 4 different donors were then pretreated with heat inactivated or anti-CA125 treated PE90 for 24 hours, followed by incubation with GMBL1 and RTX for another 24 hours before flow cytometry assay for 4-1BB. The experiments were repeated once with 3 of the 4 donor NK cells. Combined data are shown. **f**, The effect of heat inactivation and anti-CD125 antibody treatment

of patient ascites (ASC) on 41-BB expression in the ADCC-mediated NK cell activation assay. The assay was done in the same way as in **e**, except PE90 fraction was replaced with ascites. Statistical analysis was performed using one-way Anova. *p<0.05, **p<0.001, ***p < 0.0001 comparing MFI of the indicated samples.

Figure 3. CA125 concentration in ascites does not correlate with inhibition of 4-1BB up-regulation or CD16 down-regulation. **a,** Concentrations of CA125 in 22 ascites as measured by using a volume-efficient highly sensitive multiplex platform (Meso Scale Discovery) based on electrochemiluminescence (ECL) detection. The ascites samples were measured at multiple dilutions (1:10, 1:50 and 1:100). A positive quality control sample was run in duplicate on each ESL plate. **b** and **c,** Correlation analysis comparing CA125 concentrations in ascites to their effects on 4-1BB or CD16 expression (MFI) on NK cells. NK cells from three different donors were pretreated with 22 ascites at 10% concentration, followed by incubation with GMBL1 and RTX for 24 hours and flow cytometry (from Fig. 1c and 1d). MFI of 4-1BB (b) or CD16 (c) are plotted against CA125 concentration from each ascites. **d,** Correlation analysis comparing CD16 expression on NK cells to CA125 concentration. NK cells from two different donors were cultured in the presence or absence of 10% ascites for 72 hours without addition of GMBL1 cells and RTX. NK cells were then analyzed for CD16 expression by flow cytometry. CA125 concentrations in 11 ascites are plotted versus MFI of CD16 on NK cells from donor 1 and donor 2.

Figure 4. Ovarian cancer ascites specifically alters NK cell transcriptome. RNAseq was performed on NK cells from 6 healthy donors, NK cells from the same 6 healthy donors treated with ascites 1 or ascites 2, and NK cells from 6 ovarian cancer patient ascites. **a,** Principal-component analyses (PCA). **b,** Hierarchical clustering analysis of the top differentially expressed genes. Data were log transformed and scaled. Seven unique groupings were identified according to expression patterns. **c,** Enriched GO terms and pathways of significantly regulated genes between patient or ascites treated NK cells and healthy donor NK cells in clusters 1-6 shown in **b**.

Figure 5. Patient NK cells and ascites-treated NK cells show similarities in transcriptomic profiles. **a,** DEGs shared between ascites-treated NK cells and

patient NK cells. **b,** Hierarchical clustering analysis of DEGs that are either up-regulated (n = 444) or down-regulated (n = 312) in both ascites-treated NK cells and patient NK cells. **c,** Enriched GO terms and pathways of the significantly up- or down-regulated genes in both ascites-treated NK cells and patient NK cells as described in (**a**).

Figure 6. Transcriptional activation of cytotoxicity pathway is inhibited in patient NK cells and ascites-treated NK cells. **a,** Hierarchal clustering analysis of genes involved in NK cytotoxicity pathway (n = 27) that are differentially down regulated and shared between patient NK cells and ascites-treated NK cells. HD, A1, A2 and PA are the same as in Fig. 4. **b**, Quantitative PCR analysis for the transcript levels of the selected genes involved in NK cell cytotoxicity pathway. HD, A1 and PA were four of the six RNA samples used for RNAseq as described in Fig. 4. Samples of P1 fraction were RNA isolated from two healthy donor NK cells following treatment with CA125-enriched P1 fraction for 24 hours. **c,** KEGG pathway map of NK cell cytotoxicity with those genes that are down-regulated either in patient NK cells or ascites-treated NK cells indicated. Solid green bars next to the gene names indicate genes that are down regulated in ascites-treated NK cells (left) and patient NK cells (right). Open bars indicate no down-regulation in ascites-treated NK cells. The pathway image was drawn and modified by Biorender based on the KEGG pathway (hsa04650).

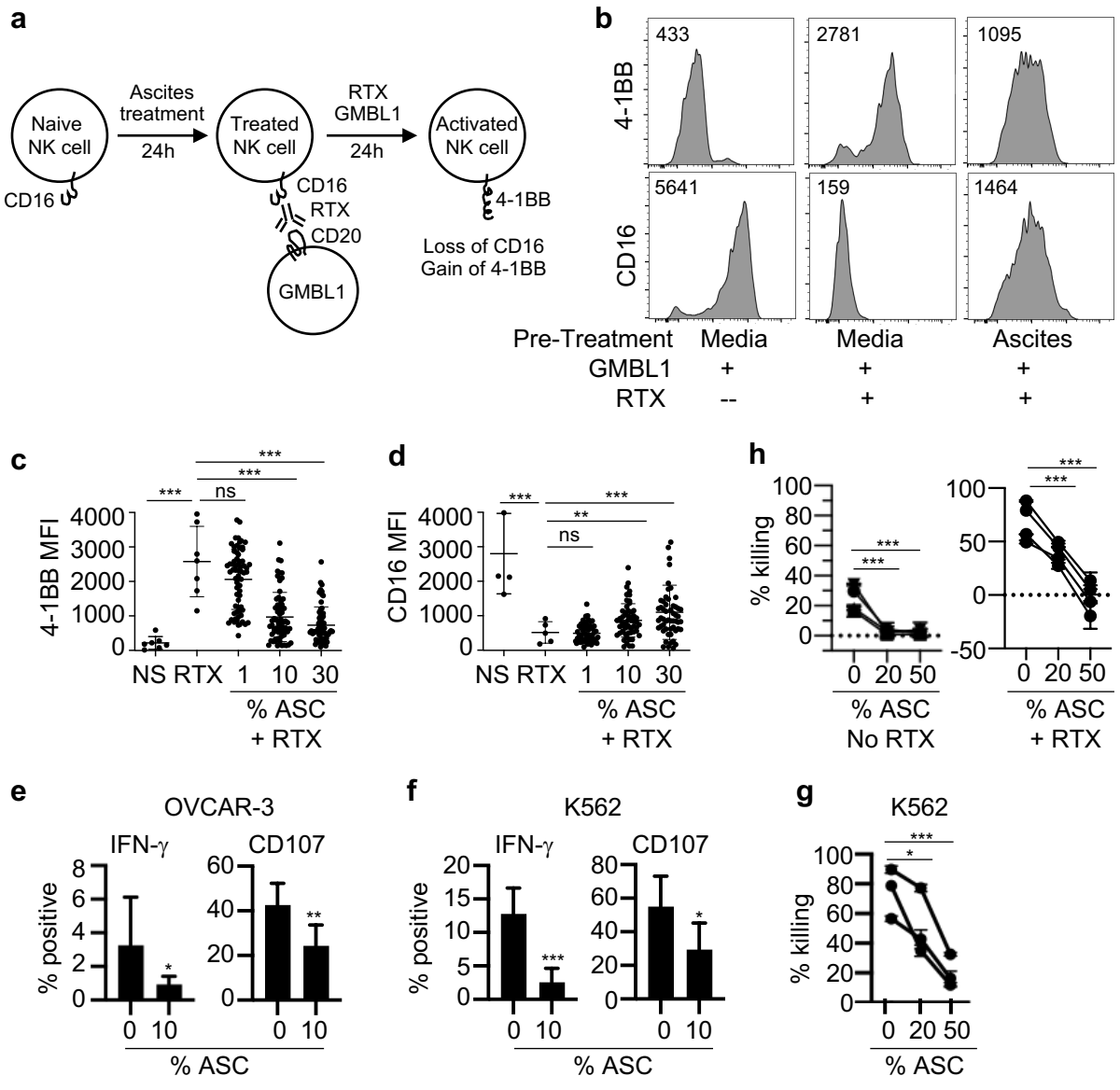
a
Naive NK cell
CD16
Ascites treatment
24h
Treated NK cell
CD16
RTX
CD20
GMBL1
RTX GMBL1
24h
Activated NK cell
4-1BB
Loss of CD16
Gain of 4-1BB
b
4-1BB
CD16
433
2781
1095
5641
159
1464
Pre-Treatment Media Media Ascites
GMBL1 + + +
RTX -- + +
c
4-1BB MFI
NS RTX 1 10 30
% ASC + RTX
d
CD16 MFI
NS RTX 1 10 30
% ASC + RTX
h
% killing
% ASC No RTX
% ASC + RTX
e
OVCAR-3
IFN-γ
CD107
% positive
% ASC
f
K562
IFN-γ
CD107
% positive
% ASC
g
K562
% killing
% ASC

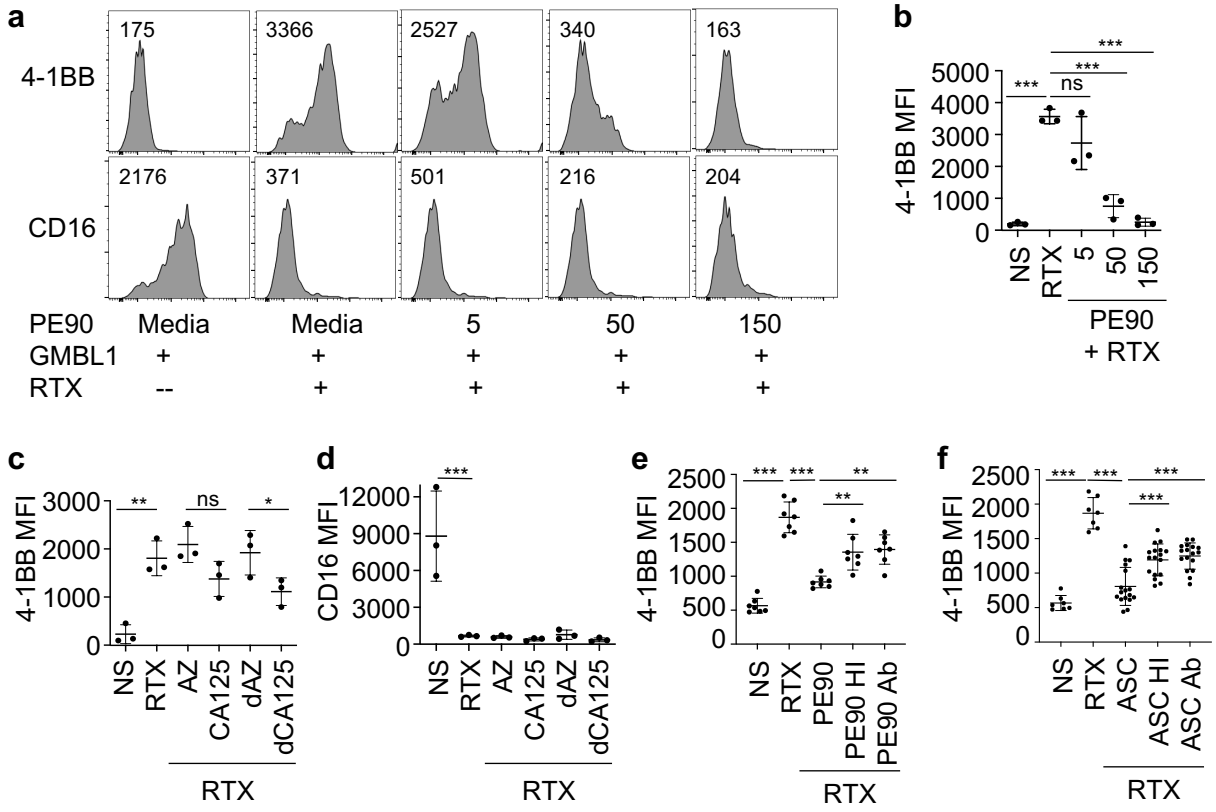
a
4-1BB
CD16
175
3366
2527
340
163
2176
371
501
216
204
PE90 Media Media 5 50 150
GMBL1 + + + + +
RTX -- + + + +
b
4-1BB MFI
5000
4000
3000
2000
1000
0
***
ns
***
***
NS
RTX
5
50
150
PE90
+ RTX
c
4-1BB MFI
3000
2000
1000
0
**
ns
*
NS
RTX
AZ
CA125
dAZ
dCA125
RTX
d
CD16 MFI
12000
9000
6000
3000
0
***
NS
RTX
AZ
CA125
dAZ
dCA125
RTX
e
4-1BB MFI
2500
2000
1500
1000
500
0
***
***
**
**
NS
RTX
PE90
PE90 HI
PE90 Ab
RTX
f
4-1BB MFI
2500
2000
1500
1000
500
0
***
***
***
***
NS
RTX
ASC
ASC HI
ASC Ab
RTX

a

Ascites	CA125 (units/mL)
DF-50	389
DF-3684	410
DF-3441	546
DF-3396	698
DF-3727	858
DF-79	916
DF-3272	1386
DF-3335	2116
DF-3400	2533
DF-3497	2856
DF-3266	2864
DF-43	3604
DF-1976	4339
DF-3095	4778
DF-22	5351
DF-21	5735
DF-3288	6920
DF-15	7571
DF-1515	16242
DF-3711	19417
DF-3191	21756
DF-3358	34296

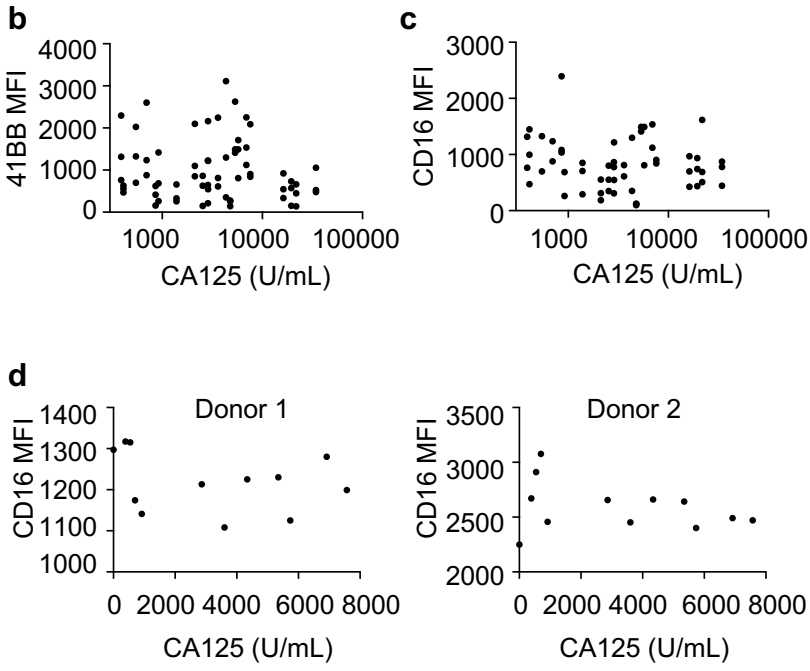

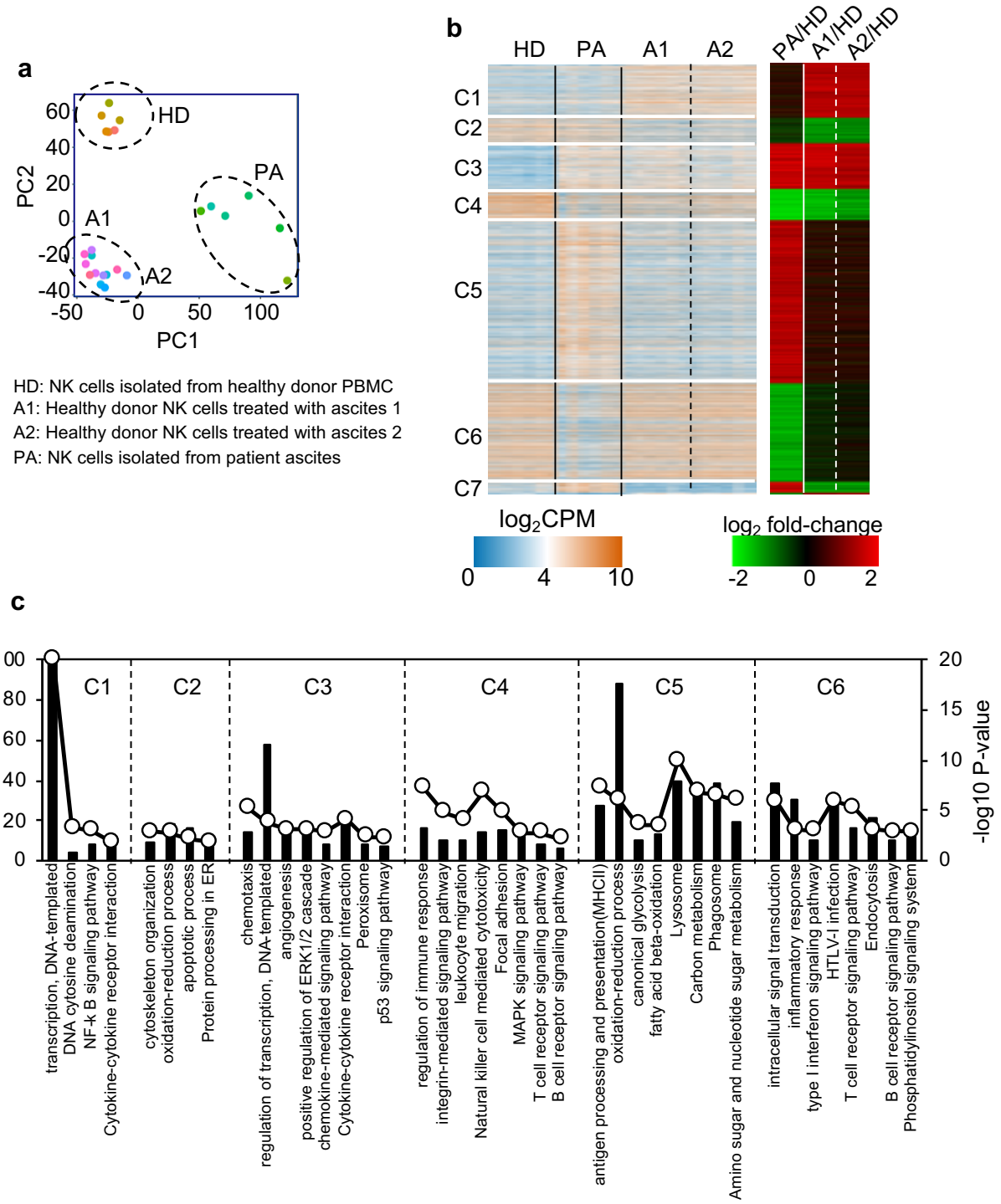
a
HD
PA
A1
A2
PC1
PC2
HD: NK cells isolated from healthy donor PBMC
A1: Healthy donor NK cells treated with ascites 1
A2: Healthy donor NK cells treated with ascites 2
PA: NK cells isolated from patient ascites
b
HD
PA
A1
A2
PA/HD
A1/HD
A2/HD
C1
C2
C3
C4
C5
C6
C7
log2CPM
log2 fold-change
c
No. of DEGs
-log10 P-value
C1
C2
C3
C4
C5
C6
transcription, DNA-templated
DNA cytosine deamination
NF-κ B signaling pathway
Cytokine-cytokine receptor interaction
cytoskeleton organization
oxidation-reduction process
apoptotic process
Protein processing in ER
chemotaxis
regulation of transcription, DNA-templated
angiogenesis
positive regulation of ERK1/2 cascade
chemokine-mediated signaling pathway
Cytokine-cytokine receptor interaction
Peroxisome
p53 signaling pathway
regulation of immune response
integrin-mediated signaling pathway
leukocyte migration
Natural killer cell mediated cytotoxicity
Focal adhesion
MAPK signaling pathway
T cell receptor signaling pathway
B cell receptor signaling pathway
antigen processing and presentation(MHCII)
oxidation-reduction process
canonical glycolysis
fatty acid beta-oxidation
Lysosome
Carbon metabolism
Phagosome
Amino sugar and nucleotide sugar metabolism
intracellular signal transduction
inflammatory response
type I interferon signaling pathway
HTLV-I infection
T cell receptor signaling pathway
Endocytosis
B cell receptor signaling pathway
Phosphatidylinositol signaling system

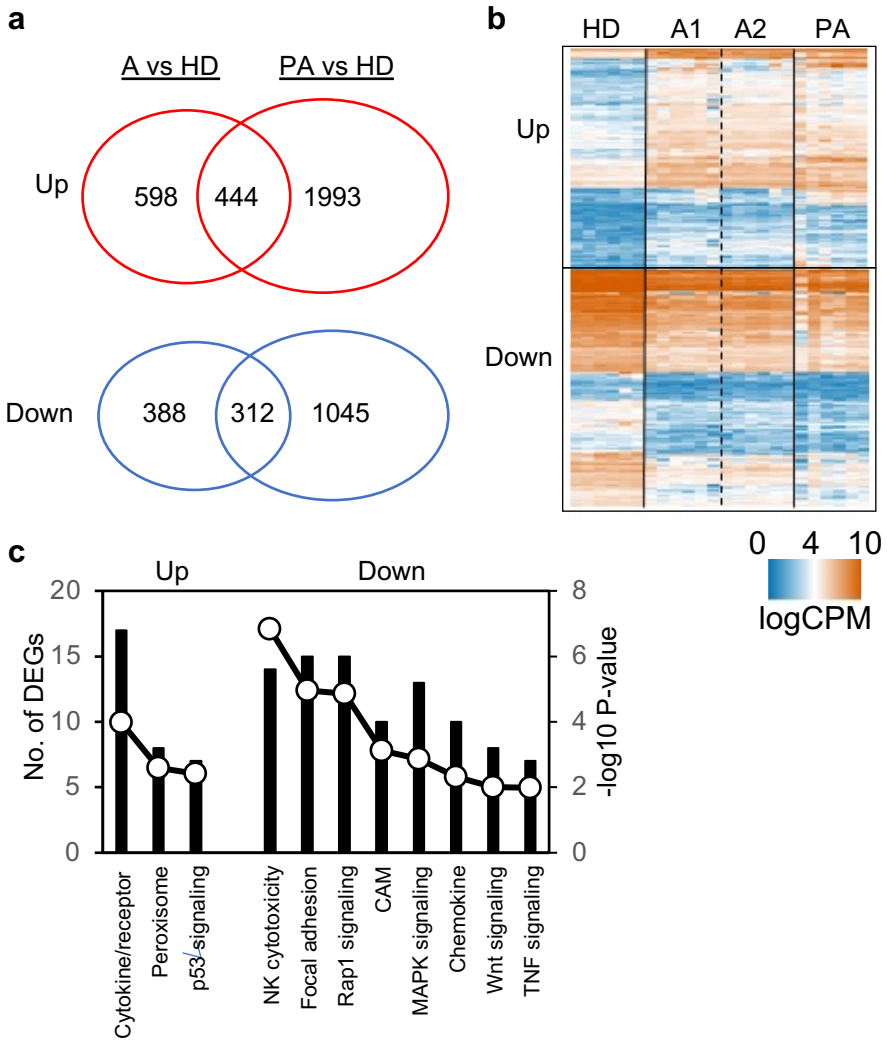
a
A vs HD
PA vs HD
Up
598
444
1993
Down
388
312
1045
b
HD
A1
A2
PA
Up
Down
0
4
10
logCPM
c
Up
Down
No. of DEGs
-log10 P-value
20
15
10
5
0
8
6
4
2
0
Cytokine/receptor
Peroxisome
p53 signaling
NK cytotoxicity
Focal adhesion
Rap1 signaling
CAM
MAPK signaling
Chemokine
Wnt signaling
TNF signaling

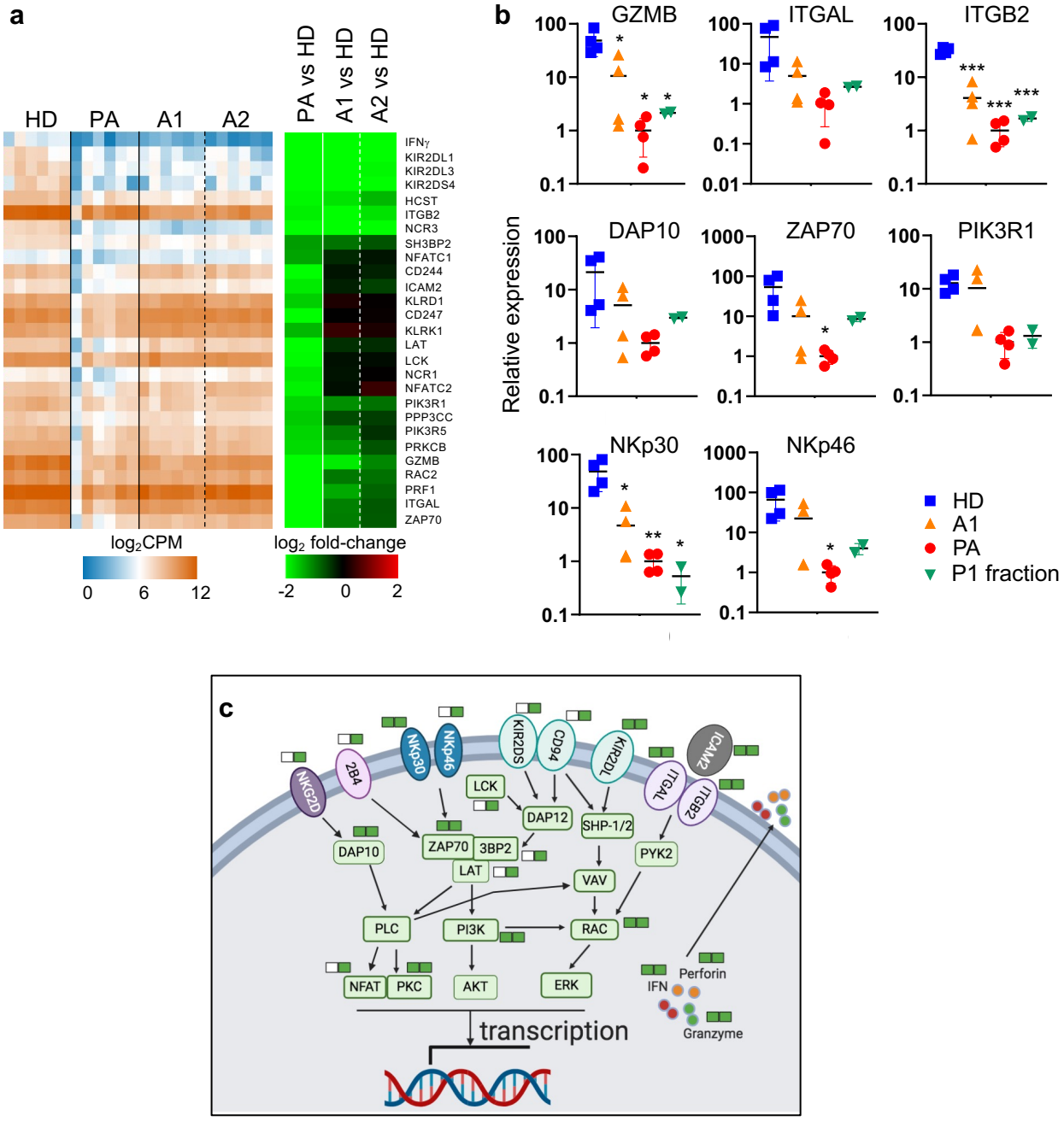
a
HD
PA
A1
A2
PA vs HD
A1 vs HD
A2 vs HD
IFNγ
KIR2DL1
KIR2DL3
KIR2DS4
HCST
ITGB2
NCR3
SH3BP2
NFATC1
CD244
ICAM2
KLRD1
CD247
KLRK1
LAT
LCK
NCR1
NFATC2
PIK3R1
PPP3CC
PIK3R5
PRKCB
GZMB
RAC2
PRF1
ITGAL
ZAP70
log2CPM
0
6
12
log2 fold-change
-2
0
2
b
GZMB
ITGAL
ITGB2
DAP10
ZAP70
PIK3R1
NKp30
NKp46
Relative expression
HD
A1
PA
P1 fraction
c
NKG2D
2B4
NKp30
NKp46
KIR2DS
CD94
KIR2DL
ICAM2
ITGAL
ITGB2
LCK
DAP12
SHP-1/2
DAP10
ZAP70
3BP2
PYK2
LAT
VAV
PLC
PI3K
RAC
NFAT
PKC
AKT
ERK
IFN
Perforin
Granzyme
transcription

Supplemental Table 1. Ovarian cancer clinical characteristics and CA125 concentration

Sample ID	CA125 (U/ml)	Age	Histologic subtype	Grade	Stage	Primary or recurrent disease	Platinum sensitive or resistant
DF-1515	16242	78	high grade serous carcinoma	not specified	IV	recurrent	resistant
DF-1976	4339	71	serous cancer of the ovary	high grade	IIIB	recurrent	resistant
DF-3095	4778	57	metastatic high grade ovarian carcinosarcoma	high grade	IIIC	recurrent	N/A
DF-3191	21756	58	high grade serous carcinoma	II of III	IV	recurrent	resistant
DF-3266	2864	82	metastatic adenocarcinoma of Mullerian origin	N/A	N/A	primary	N/A
DF-3272	1386	77	Metastatic serous adenocarcinoma	High grade	N/A	primary	N/A
DF-3288	6920	60	high grade serous carcinoma	not specified	IIIc	primary	sensitive
DF-3335	2116	67	Metastatic serous adenocarcinoma	High grade	Advanced	recurrent	resistant
DF-3358	34296	60	high grade serous carcinoma	not specified	IV	recurrent	resistant
DF-3396	698	N/A	Endometriod adenocarcinoma	Low grade (I)	III	recurrent	N/A
DF-3400	2533	59	metastatic ovarian carcinosarcoma	high grade	IIIC	recurrent	resistant
DF-3441	546	63	Mullerian carcinoma of the ovary	High grade	III	primary	N/A
DF-3497	2856	67	high grade ovarian serous carcinoma	high grade	IIIC	recurrent	resistant
DF-3684	410	63	Poorly differentiated carcinosarcoma of the uterus	N/A	IA	primary	N/A
DF-3711	19417	68	poorly differentiated mullerian carcinoma	not specified	IVa	primary	sensitive
DF-3727	858	68	Metastatic serous adenocarcinoma	High grade	N/A	primary	N/A
DF-15	7571	52	Papillary serous adenocarcinoma	N/A	IIIc	N/A	N/A
DF-21	5735	52	Serous papillary carcinoma	N/A	III	N/A	N/A
DF-22	5351	N/A					
DF-43	3604	N/A					
DF-50	389	N/A					
DF-79	916	N/A					

N/A, not available.

Supplemental Table 2. Inhibitory factors in patient ascites.

Ascites sample	CA125 units/mL	MICA pg/mL	MICB pg/mL	IL-10 pg/mL	TGF-β pg/mL	41BB MFI	CD16 MFI
DF-50	389.4	ND	143	906.17	3460	763	646
DF-3441	546.2	ND	171.5	981.17	1560	698	662
DF-3396	698.3	ND	128.5	171.17	ND	878	916
DF-79	916.5	ND	60.5	0	160	260	1107
DF-3266	2863.7	ND	944.5	272.83	1310	545	1149
DF-43	3604.2	ND	205.5	877.83	3560	611	817
DF-1976	4339.4	ND	189	477.83	8960	350	860
DF-22	5350.8	ND	844.5	169.5	4960	1492	483
DF-21	5734.9	ND	188.5	222.83	3160	808	636
DF-3288	6919.8	ND	1299	364.5	2160	1122	533
DF-15	7570.9	ND	343	1212.83	4810	904	988

MFI of 4-1BB and CD16 were from NK cells that were pretreated with 10% ascites and then cultured with GMBL1 and RTX for 24 hours. ND, not detectable.

Supplemental Table 3. Enriched GO terms and pathways of transcripts identified in the group clusters in Figure 4C.

	Term	Count	PValue	LogP
C1	GO:0006351~transcription, DNA-templated	100	1.57E-30	-29.803026
	GO:0070383~DNA cytosine deamination	4	4.70E-04	-3.3278121
	hsa04064:NF-kappa B signaling pathway	8	9.24E-04	-3.034351
	hsa04060:Cytokine-cytokine receptor interaction	11	0.0120518	-1.9189472
C2	GO:0007010~cytoskeleton organization	9	0.0011488	-2.9397531
	GO:0055114~oxidation-reduction process	18	0.0017216	-2.7640756
	GO:0006915~apoptotic process	16	0.0067148	-2.1729698
	hsa04141:Protein processing in ER	8	0.0118559	-1.9260659
C3	GO:0006935~chemotaxis	14	5.52E-06	-5.2580388
	GO:0006355~regulation of transcription, DNA-templated	58	1.75E-04	-3.7568661
	GO:0001525~angiogenesis	15	7.88E-04	-3.1034466
	GO:0070374~positive regulation of ERK1/2 cascade	13	8.53E-04	-3.0692277
	GO:0070098~chemokine-mediated signaling pathway	8	0.0013186	-2.8799032
	hsa04060:Cytokine-cytokine receptor interaction	18	8.27E-05	-4.0823234
	hsa04146:Peroxisome	8	0.003996	-2.3983699
	hsa04115:p53 signaling pathway	7	0.0056554	-2.2475392
C4	GO:0050776~regulation of immune response	16	5.43E-08	-7.2653757
	GO:0007229~integrin-mediated signaling pathway	10	1.43E-05	-4.8447064
	GO:0050900~leukocyte migration	10	7.54E-05	-4.1228223
	hsa04650:Natural killer cell mediated cytotoxicity	14	1.59E-07	-6.7975317
	hsa04510:Focal adhesion	15	1.22E-05	-4.9136373
	hsa04010:MAPK signaling pathway	13	0.0014562	-2.8367684
	hsa04660:T cell receptor signaling pathway	8	0.0017294	-2.7621056
	hsa04662:B cell receptor signaling pathway	6	0.0068639	-2.1634302
C5	GO:0019886~antigen processing and presentation(MHCII)	27	4.95E-08	-7.3057395
	GO:0055114~oxidation-reduction process	88	9.85E-07	-6.0065069
	GO:0061621~canonical glycolysis	10	2.34E-04	-3.6307862
	GO:0006635~fatty acid beta-oxidation	13	2.91E-04	-3.5364386
	hsa04142:Lysosome	40	1.01E-10	-9.9964366
	hsa01200:Carbon metabolism	33	1.57E-07	-6.8037302
	hsa04145:Phagosome	39	2.71E-07	-6.5663944
	hsa00520:Amino sugar and nucleotide sugar metabolism	19	9.767E-07	-6.0102568
C6	GO:0035556~intracellular signal transduction	39	1.06E-06	-5.9765418
	GO:0006954~inflammatory response	30	7.47E-04	-3.1267897
	GO:0060337~type I interferon signaling pathway	10	1.00E-03	-3.0000809
	hsa05166:HTLV-I infection	28	1.23E-06	-5.9115172
	hsa04660:T cell receptor signaling pathway	16	5.24E-06	-5.2807093
	hsa04144:Endocytosis	21	9.02E-04	-3.0450336
	hsa04662:B cell receptor signaling pathway	10	0.0011858	-2.9259728
	hsa04070:Phosphatidylinositol signaling system	12	0.0012494	-2.9032958

Supplemental Table 4. Enriched GO terms and pathways of transcripts identified in the groups clusters in Figure 5C.

	Term	Count	PValue	LogP
Up	GO:0006935~chemotaxis	13	1.70E-05	-4.77
	GO:0006355~regulation of transcription, DNA-templated	57	7.82E-05	-4.11
	GO:0001525~angiogenesis	15	4.65E-04	-3.33
	GO:0070098~chemokine-mediated signaling pathway	8	9.74E-04	-3.01
	GO:0042059~negative regulation of epidermal growth factor receptor signaling pathway	5	7.98E-03	-2.10
	GO:0006915~apoptotic process	22	1.53E-02	-1.81
	GO:0070374~positive regulation of ERK1 and ERK2 cascade	10	1.62E-02	-1.79
	GO:0043123~positive regulation of I-kappaB kinase/NF-kappaB signaling	9	2.72E-02	-1.57
	GO:0006914~autophagy	8	2.87E-02	-1.54
Down	GO:0050776~regulation of immune response	16	3.89E-08	-7.41
	GO:0007229~integrin-mediated signaling pathway	10	1.17E-05	-4.93
	GO:0032870~cellular response to hormone stimulus	7	4.00E-05	-4.40
	GO:0007155~cell adhesion	18	3.22E-04	-3.49
	GO:0050900~leukocyte migration	9	3.58E-04	-3.45
	GO:0051591~response to cAMP	6	4.77E-04	-3.32
	GO:0045944~positive regulation of transcription from RNA polymerase II promoter	28	7.87E-04	-3.10
	GO:0045595~regulation of cell differentiation	5	1.05E-03	-2.98
	GO:0007165~signal transduction	30	2.23E-03	-2.65
	GO:0032526~response to retinoic acid	5	2.68E-03	-2.57
	GO:0050852~T cell receptor signaling pathway	7	1.93E-02	-1.71
	GO:0002250~adaptive immune response	7	1.93E-02	-1.71
	GO:0030198~extracellular matrix organization	8	2.24E-02	-1.65
	GO:0006468~protein phosphorylation	13	3.07E-02	-1.51
	GO:0051607~defense response to virus	7	3.10E-02	-1.51
	GO:0006955~immune response	12	3.88E-02	-1.41

Supplemental Table 5. Primer sequences for gene expression analysis by quantitative PCR (qRT-PCR).

Gene	Forward	Reverse	Coding DNA Length
DAP10	TCTGGGTCACATCCTCTTCCT	AAGTGCCAGGGTAAAAGGCAG	279
ITGAL	TGCTTATCATCATCACGGATGG	CTCTCCTTGGTCTGAAAATGCT	3261
ITGB2	TGCGTCCTCTCTCAGGAGTG	GGTCCATGATGTCGTCAGCC	2310
NKp46	TGGACCCGAAGTGATCTCG	TCCTTGAGCAGTAAGAACATGC	579
NKp30	CCCCTGAGATTCGTACCCTG	CTCCACTCTGCACACGTAGAT	573
ZAP70	CGAGCGTGTATGAGAGCCC	ATGAGGAGGTTATCGCGCTTC	939
PIK3R1	ACCACTACCGGAATGAATCTCT	GGGATGTGCGGGTATATTCTTC	2175
GZMB	CCCTGGGAAAACACTCACACA	GCACAACTCAATGGTACTGTCG	744

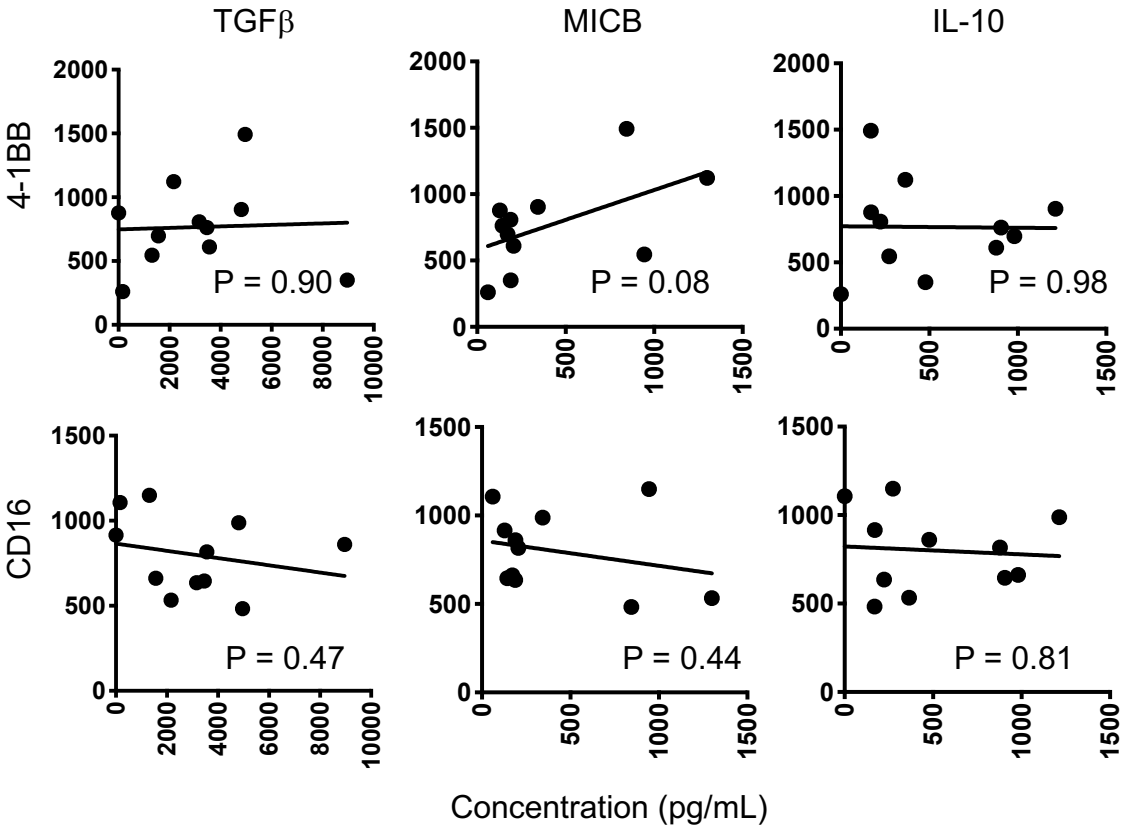

Supplemental Figure 1. Correlation between the levels (MFI) of 4-1BB (upper) or CD16 (lower), after incubation with 10% ascites prior to stimulation, with the concentrations of TGF-β, MICB and IL-10 in the ascites as measured by ELISA. P value and slope were determined by linear regression analysis.

a

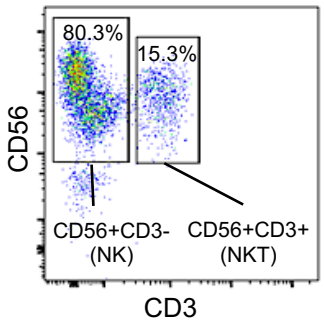

b

Ascites donor	CD56+ cells (x 10^6)	% NK	% NKT
DF1111	0.57	80.3	15.3
DF1112	0.25	69.7	30.2
DF3856	0.93	85.5	13.6
DF3481	0.27	75.4	22.9
DF3706	0.65	67.0	32.1
DF3459	0.83	59.4	29.1

Supplemental Figure 2. **(a)** A representative flow cytometry analysis of NK cells purified from ascites of an ovarian cancer patient. NK cells were purified using immunomagnetic negative selection. Isolated NK cells were stained with antibodies specific for CD56 and CD3, followed by flow cytometry. Shown are CD3 versus CD56 staining profiles gating on live cells (DAPI-). **(b)** Summary of the number and purity of NK cells purified from 6 patient ascites. Percent NK and percent NKT cells were calculated after gating on live cells (DAPI-) and setting regions around CD56+CD3- NK cells and CD56+CD3+ NKT cells as shown in a.

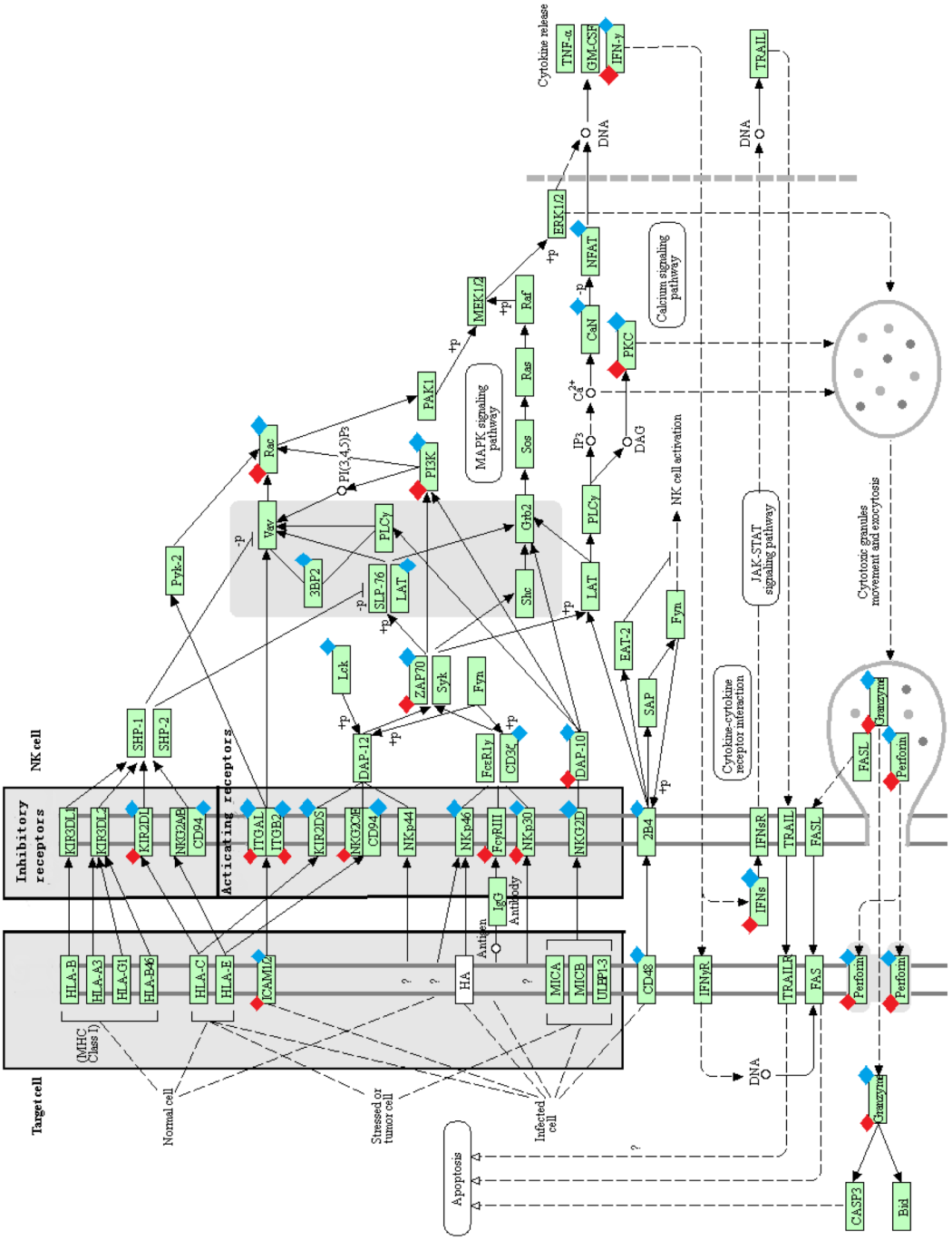

Supplemental Figure 3. The more extensive KEGG pathway analysis of genes involved in NK cell cytotoxicity. Red diamonds indicate genes that were down-regulated in ascites-treated NK cells as compared to healthy donor NK cells. Blue diamonds indicate genes that were down-regulated in patient NK cells as compared to healthy donor NK cells.